Adv Polym Sci (2016) 270: 29–76
DOI: 10.1007/12_2015_311

Published online: 20 May 2015

Surface-Initiated Atom Transfer Radical Polymerization

Amir Khabibullin, Erlita Mastan, Krzysztof Matyjaszewski, and Shiping Zhu

Abstract This review covers the basic principles of surface-initiated atom transfer radical polymerization (SI-ATRP). SI-ATRP is a robust and versatile method for preparation of various hybrid materials with controlled molecular characteristics of the tethered polymer chains, such as polymer composition and architecture. Various aspects of SI-ATRP, such as polymer brush grafting density, surface geometry, and reaction conditions, including structure of initiator, ligand, and catalyst, are important for engineering the structure and properties of the hybrid polymer materials. Elementary reactions, such as initiation, propagation, termination, transfer, and activation/deactivation equilibria as well as factors affecting these processes are discussed. The properties of materials prepared by SI-ATRP are illustrated through several selected examples.

Keywords Controlled radical polymerization · Elementary reactions · Mechanism · Grafting density · Surface geometry

Contents

A. Khabibullin and K. Matyjaszewski (✉)
Department of Chemistry, Carnegie Mellon University, Pittsburgh, PA 15213, USA
e-mail: km3b@andrew.cmu.edu

E. Mastan and S. Zhu (✉)
Department of Chemical Engineering, McMaster University, 1280 Main Street West, Hamilton, ON, Canada, L8S 4L7
e-mail: zhuship@mcmaster.ca

1 ATRP Fundamentals

Controlled radical polymerization (CRP, also termed reversible-deactivation radical polymerization, RDRP) is a versatile method for the preparation of well-defined polymers [1]. Unlike conventional radical polymerization with its slow continuous initiation, fast propagation, and inevitable radical termination, CRP creates and exploits a dynamic equilibrium between growing radicals and dormant species [2]. In this system, the active radicals are deactivated after adding one or several monomer units and converted back to the dormant state. This approach allows preparation of polymers with precise control over molecular weight (MW), molecular weight distribution (MWD), polymer composition, topology, and functionality.

Atom transfer radical polymerization (ATRP) is one of the most robust and widely used CRP techniques for polymerization of a broad range of commercially available functional monomers [3–5]. It is attractive because of the simple experimental setup, with readily available initiators and catalysts that can be used in a range of solvents under a broad spectrum of reaction conditions, allowing precise control over final polymer MW and architecture [6].

In ATRP, the dormant species are either low MW initiating alkyl halides or a macromolecular species (P_n-X). The dormant species intermittently react with activators and deactivators. Activators are, typically, ligand-stabilized transition metal complexes in their lower oxidation states (M^m/L), that react with the dormant species to form active radicals ($P_n^{\bullet}$). Deactivators are usually transition metal complexes in their higher oxidation state, coordinated with the transferred halide ligands (X-M^{m+1}/L). After adding a few monomer units, the growing radical then reacts with a deactivator to re-form a dormant species and regenerate the activator. Radicals also terminate, as in any radical polymerization. Scheme 1 illustrates a typical ATRP equilibrium.

Scheme 1 ATRP equilibrium

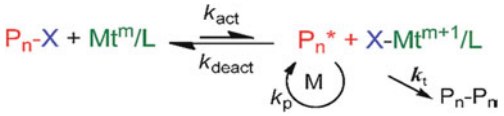

The rate of ATRP (R_p) depends on the propagation rate constant (k_p) and on the concentrations of monomer and growing radical. The concentration of the growing radical depends on the ATRP equilibrium constant, as well as on the concentrations of the dormant species, activators, and deactivators, as shown in the ATRP rate equation given below. The equilibrium constant K_{ATRP} is equal to k_{act}/k_{deact} and depends on the strength of both the C–X and the Cu^{II}–X bonds. The equilibrium constant increases with the strength of the Cu^{II}–X bonds, or the halogenophilicity of the Cu^{I} complex, and decreases with the strength of the C–X bonds.

$$R_p = k_p[M]\left[P_n^*\right] = k_p K_{ATRP}\left(\frac{[P_nX][Cu^IL][M]}{[X\text{-}Cu^{II}L]}\right) \quad \text{(ATRP equation)}$$

ATRP is a catalytic process and can be mediated by many redox-active transition metal complexes. The most frequently used metal is Cu; however, ATRP has also been successfully carried out using Ru, Fe, Mo, Os, etc. [7]. The key limitation of "normal" ATRP (as it was initially defined) is the large amount of catalyst loading (up to ca. 1 mol%) compared with monomer. This residual metal creates difficulties in purification of the final product [8]. Also, in ATRP, as in any radical process, radical termination occurs but involves only about 1–10% of all chains. Radical termination leads to irreversible transformation of a fraction of the activator to deactivator, leading to a decrease in the reaction rate.

However, according to the equation given above, the ATRP rate does not depend on the absolute catalyst concentration, but rather on the ratio of the concentrations of activator and deactivator. Several novel ATRP techniques have been developed exploiting this feature, eliminating the problem of high catalyst loading and a slowdown in the rate of polymerization as a result of radical termination [9]. These novel low catalyst concentration procedures include activators regenerated by electron transfer (ARGET)-ATRP [10], initiators for continuous activator regeneration (ICAR)-ATRP [11], supplemental activator and reducing agent (SARA)-ATRP [12–14], photochemically mediated ATRP [15–19], and eATRP, where the activator/deactivator ratio is controlled electrochemically [20–22]. These recent developments are summarized in Scheme 2, which also summarizes the possibilities for engineering macromolecular architecture provided by ATRP, as well as a few of the targeted applications for the resulting materials [23].

The appropriate choice of initiator and ligand and their amounts are important for preparation of the desired product in a controlled manner [24–26]. The selected alkyl halide initiators should possess sufficient reactivity for efficient initiation of polymerization of the selected monomers, which correspondingly depends on the structure of the alkyl group and the transferable halogen or pseudohalogen [27]. The reactivities of the halides follow the order tertiary > secondary > primary carbon atom, according to the change in bond dissociation energy needed for

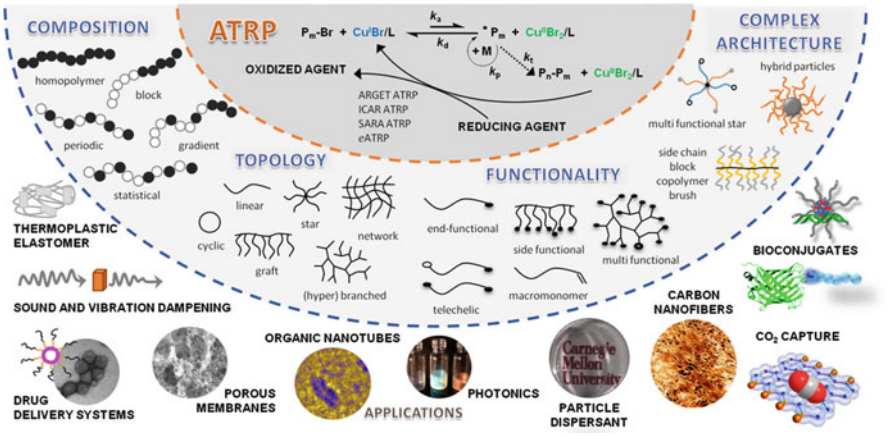

Scheme 2 Overview of recent advances in ATRP that allow a reduction in catalyst loading, down to part per million levels, and engineering of macromolecular architecture. Applications for some of the resulting materials are shown. Reprinted with permission from Matyjaszewski and Tsarevsky [23]

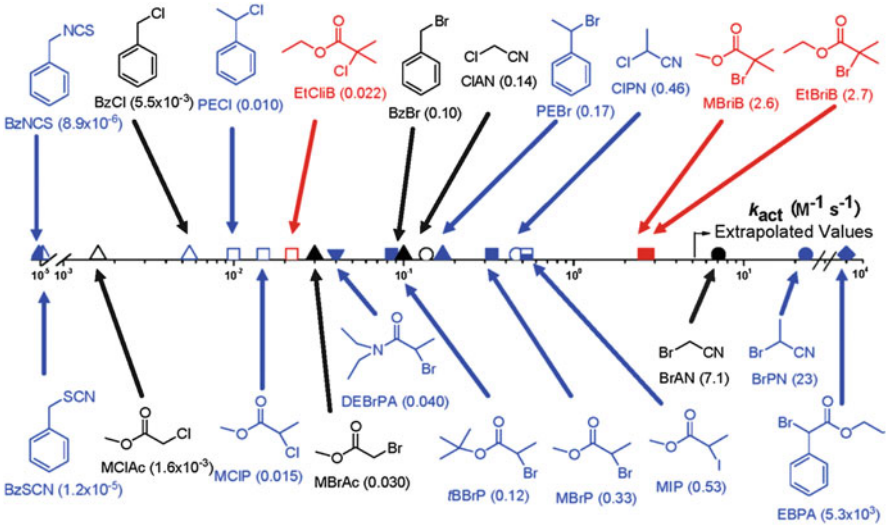

Scheme 3 ATRP activation rate constants for various initiators with $Cu^{I}X$/PMDETA (where X=Br or Cl) in MeCN at 35°C. 3° initiators are in *red*; 2° *blue*; 1° *black*; with isothiocyanate/thiocyanate *half-filled triangle*; chloride *open symbols*; bromide *filled symbols*; iodide *half-filled square*; amide ▼; benzyl ▲; ester □; nitrile ○; phenyl ester ◇. Reprinted with permission from Tang and Matyjaszewski [27]

homolytic bond cleavage. Also, the reactivities of alkyl halides follow the order I ~ Br > Cl and are higher than the reactivity of alkyl pseudohalides. The ATRP activation rate constants for various initiators are shown in Scheme 3

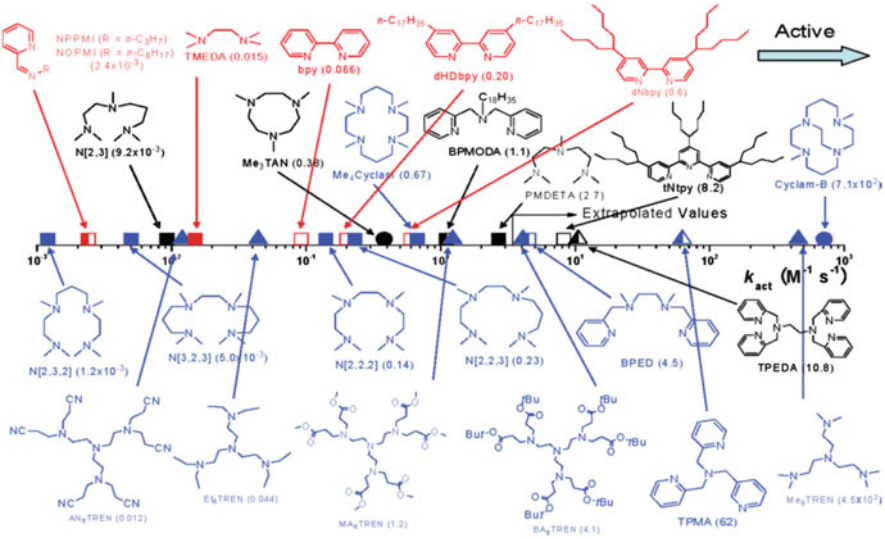

Scheme 4 ATRP activation rate constants for various ligands with EtBriB in the presence of CuIBr in MeCN at 35°C. Compounds with two nitrogen atoms (N2) *red*; N3 *black*; N4 *blue*; amine/imine *filled symbols*; pyridine *open symbols*; mixed *left-half filled symbols*; linear □; branched ▲; cyclic ○. Reprinted with permission from Tang and Matyjaszewski [29]

The effect of the selected ligand on the ATRP rate constant is profound, and the range of activity of the formed copper-based ATRP catalyst complexes covers six orders of magnitude [26, 28, 29]. Generally, Cu complex activity in ATRP for ligands follows the order tetradentate (cyclic-bridged) > tetradentate (branched) > tetradentate (cyclic) > tridentate > tetradentate (linear) > bidentate. The activity of ligands for ATRP also depends on the nature of the nitrogen atom and follows the order aliphatic amine > imine > aromatic amine. Steric effects are also very important. The ATRP activation rate constants for Cu complexes with various ligands are shown in Scheme 4.

There are several other factors in ATRP that affect polymerization control and properties of the final product in addition to choice of initiator and ligand. The polymerization media plays a significant role in the process. ATRP can be conducted in bulk, solution, or in a variety of heterogeneous media including microemulsions, miniemulsions, emulsions, suspensions, dispersions, and inverse miniemulsions. The choice of media primarily depends on solubility or heat transfer considerations; for example, conditions have to be selected so that the catalyst complex and the product are at least partially soluble in the reaction medium. ATRP is strongly accelerated in the presence of more polar solvents [30], and at higher temperatures [31] and pressures [32].

Surface-initiated ATRP (SI-ATRP) follows the same mechanism and is controlled by the same factors as a regular ATRP; however, there are several unique requirements, which are discussed in detail in Sect. 4.

2 Hybrid Materials

Hybrid materials consist of two or more disparate components connected at molecular level, most often by covalent bonds. Typical hybrid systems are formed by attaching organic polymers to an inorganic substrate (organic/inorganic hybrids), linking synthetic polymers to natural products, or combining polymer fragments prepared by different polymerization techniques. Hybrid materials represent a rapidly growing area of molecularly designed materials, and ATRP has contributed significantly to its development. Polymers synthesized using ATRP can provide important desired properties to hybrid materials, including solubility in different phases of a biphasic system, responsiveness to stimuli, functionality, and mechanical strength.

The three widely used methods used to create hybrid materials containing polymer segments are grafting-from, grafting-onto, and grafting-through. Another method for hybrid material synthesis was introduced recently, the template approach.

2.1 "Grafting From" Approach

The grafting-from approach provides a versatile and efficient tool for creating functional hybrid materials. It includes surface-initiated CRP (SI-CRP) and, particularly, SI-ATRP, which is widely used to graft polymers from substrate surfaces [33, 34]. The advantages of the grafting-from approach using ATRP include a high level of control over polymer graft architecture and grafting density, as well its applicability to various substrate surface geometries (flat surfaces, nanoparticles, inside the pores, etc.) and compositions, including metals and metal oxides, silicon, organic polymers, and natural products. Ultimately, (co)polymers with a very high graft density form polymeric brushes [35].

The key requirement for the grafting-from approach is the presence of polymerization initiators that are covalently attached and evenly distributed throughout the substrate surface. The polymer chains are then grown from the surface of the substrate. The initiator can either be an inherent part of the substrate (e.g., some polymers carrying functional groups) or can be introduced to the substrate surface via an additional surface functionalization reaction. One can precisely control the grafting density and, if desired, introduce densely grafted brushes to the surface. Scheme 5 illustrates the grafting-from approach using SI-ATRP.

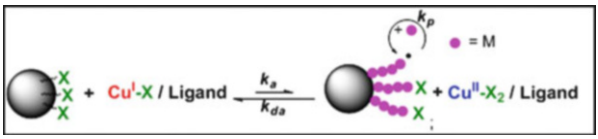

Scheme 5 Grafting-from approach employed to introduce polymer brushes onto the surface of a nanoparticle via SI-ATRP

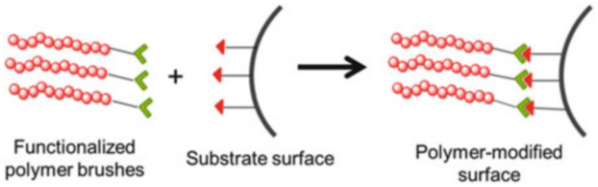

Scheme 6 Grafting-onto approach using "click" chemistry

2.2 *"Grafting-Onto" Approach*

In this method, one needs to prepare polymer chains with end-functional groups and then covalently link the polymer chains to the substrate surface. The substrate surface should have corresponding complementary functional groups, which can either be an inherent part of the substrate, for instance, the hydroxyl groups on the surface of metal oxides, or can be introduced separately. However, this method is often limited by steric hindrance and slow diffusion of bulk polymer chains to the substrate surface [36]. Although this high-yield grafting-onto method gained increased attention with the development of "click" chemistry, which allows fast and quantitative linking of functionalized chains to corresponding surface functional groups via Cu-catalyzed reaction between alkynes and azides [37, 38], the grafting density is much lower than that attained in grafting-from procedures as a result of steric crowding and entropic effects.

Scheme 6 illustrates the grafting-onto approach using click chemistry.

2.3 *"Grafting-Through" Approach*

In order to utilize the grafting-through approach, the substrate first needs to be modified with a polymerizable monomer unit, thus becoming a hybrid "macromonomer." The macromonomer is then copolymerized with low molecular weight monomers to form a polymer chain with "sewed" substrate moieties. This method is illustrated in Scheme 7.

This method permits preparation of hybrid materials using macromonomers that can be inorganic, natural products, or other polymers, either prepared by CRP or any other polymerization technique. The grafting density and number of grafted chains depend on the ratio of the concentrations of monomer and macromonomer

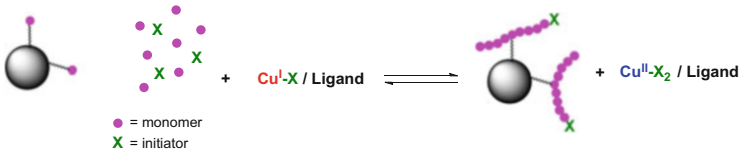

Scheme 7 Grafting-through approach for introduction of polymer brushes to the surface of nanoparticles using ATRP

but are generally much lower than obtained using grafting-onto or grafting-from procedures.

2.4 Templated Approach

Inorganic particles (spheres and cylinders) are often prepared using surfactants that form templating micelles [39–42]. Polymer chemistry provides an easy approach for preparation of unimolecular micelles of predefined structure such as molecular brushes [43–45] or stars [46, 47], which can serve as templates for the preparation of silica [39, 40], titania [48, 49], or gold [41, 42] nanoparticles. The polymer templating approach can also be used for preparation of ordered honeycomb structures of Pd and other heavy metals [50]. The emerging templating techniques use core–shell brushes [40] or star-like block copolymers [51] as nanoreactors, providing facile and versatile tools for synthesis of well-defined nanocrystals with uniform controlled size, composition, and architecture.

For example, Scheme 8 summarizes the strategy for the preparation of silica nanowires using a polymer brush template approach. First, a poly (3-acryloylpropyltrimethoxysilane) (APTS) block was grafted from linear multifunctional initiator, that is, a linear polymer backbone carrying ATRP initiating sites. Each APTS block was then chain-extended with an oligo(ethylene glycol) methacrylate (OEGMA) block, thus creating a cylindrical polymer brush with a cylindrical APTS core and an OEGMA shell. The APTS core block was then crosslinked, forming a hybrid organo-silica nanowire. The hybrid nanowire can be further transformed to a fully inorganic silica nanowire via pyrolysis of the organic segment at 700°C.

The star-polymer template approach allows preparation of spherical nanocrystals. In the initial step, a star-like block copolymer nanoreactor was prepared, with a polyacrylic acid (PAA) inner block and an outer block of polystyrene. Then, the inner PAA block was infiltrated with the precursor for preparation of the desired nanoparticles. Finally, the precursor is transformed into the nanoparticle inside the star-polymer template, resulting in formation of uniform well-defined nanocrystals. By using a star-like triblock copolymer template, core–shell and hollow nanocrystals can be prepared following similar strategies (Scheme 9).

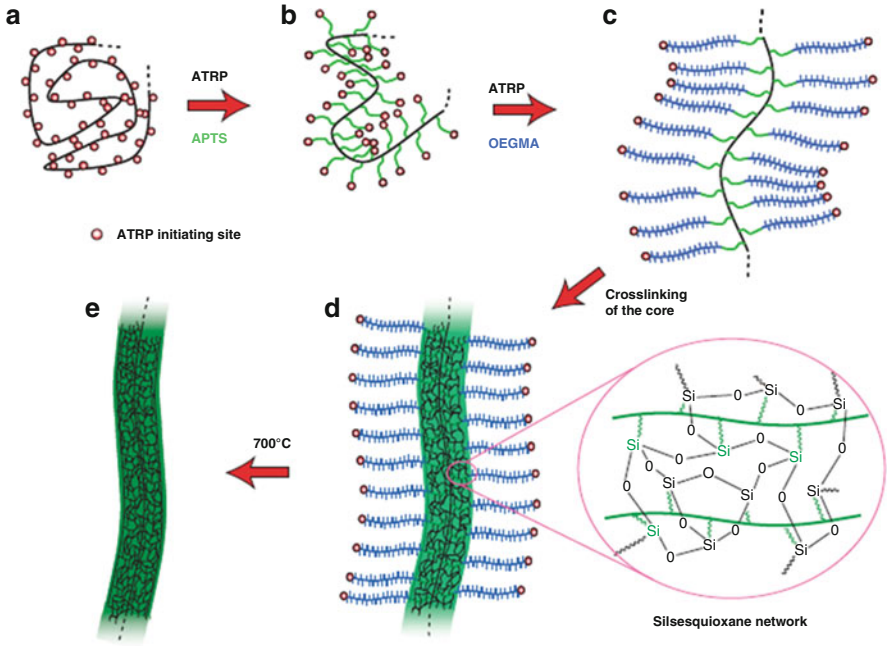

Scheme 8 Synthesis of a silica nanowire using the polymer brush template approach. (**a**) ATRP multi-initiator poly[2-(2-bromoisobutyryloxy)ethyl methacrylate] (PBIEM) with degree of polymerization of 3,200; (**b**) cylindrical polymer brush (CPB) with side chains of 20 APTS units; (**c**) core–shell CPB with an additional 57 OEGMA units; (**d**) soluble organo-silica hybrid nanowires with a crosslinked silsesquioxane network in the core; (**e**) inorganic silica nanowires after pyrolysis. Reprinted with permission from Yuan et al. [40]

Depending on the precursor used, the resulting nanocrystals can provide different functionalities (e.g., they can be metallic, magnetic, semiconductor, or fluorescent).

3 SI-ATRP

3.1 Selection of Surface Geometry

SI-ATRP can be carried out on wide variety of surfaces, including flat surfaces, nanoparticles, cylindrical surfaces, or on the surface inside nanopores. The presence of ATRP initiator is the only requirement for successful introduction of polymer brushes via SI-ATRP. However, the choice of surface geometry can influence the parameters controlling the architecture of the grafted polymer brushes. For example, the grafting density for polymer brushes on a flat surface is usually below 0.5 chain/nm^2, whereas convex systems, such as functionalized nanoparticles, can have a significantly higher grafting density, approaching 1 chain/nm^2. However,

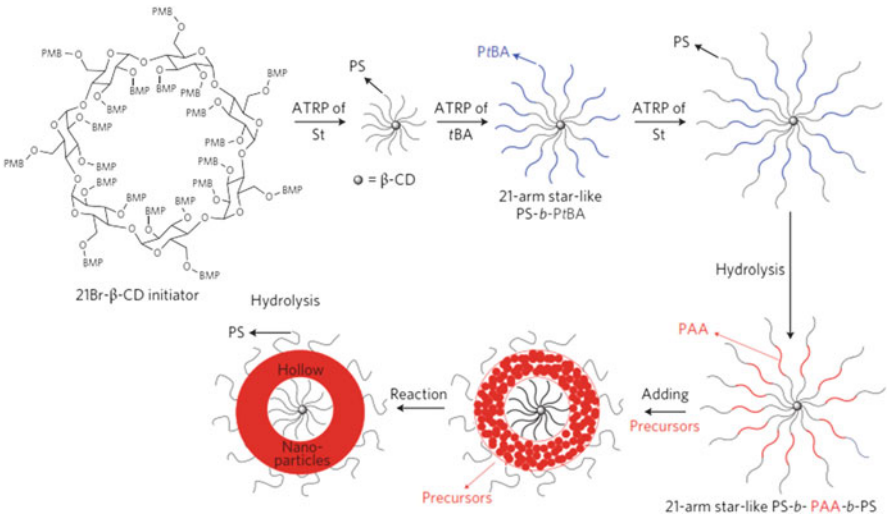

Scheme 9 Synthesis of hollow hybrid nanoparticles using the star-polymer template approach. Reprinted with permission from Pang et al. [51]

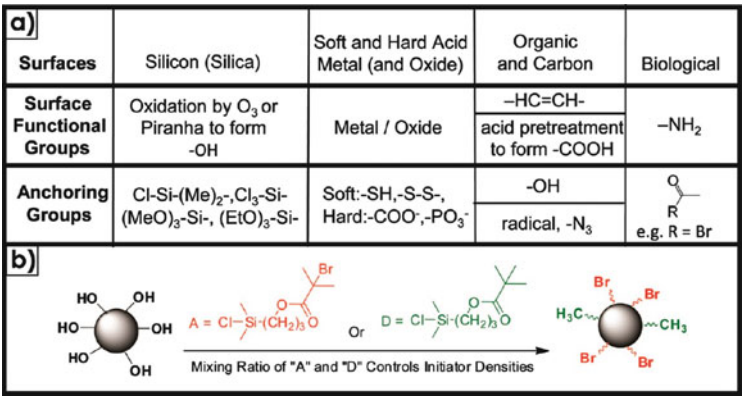

Scheme 10 (**a**) Examples of functional groups for modification of various surfaces. (**b**) Strategy for controlling grafting density using the active/inactive initiator approach. Reprinted with permission from Hui et al. [34]

such systems are prone to macroscopic gelation, even at only 0.1% of interparticle radical termination. In concave systems (e.g., inside cylindrical or spherical pores), steric hindrance plays a significant role, reducing the level of control over polymer brush MW and MWD. However, in some systems good control was reported [52]. Details of the effect of surface geometry on grafting polymers via SI-ATRP are discussed further in Sect. 4.

3.2 Selection of Substrate

A suitable substrate material can be selected depending on the desired application of the final functional material. SI-ATRP allows growth of polymer chains from the surface of metals, metal oxides, silicon, quantum dots, and a variety of organic polymers and biological species. The only requirement is that the initiator moieties are covalently attached to each substrate via the corresponding anchoring groups. Scheme 10a shows examples of anchoring groups for different substrate materials.

3.3 Advantages of SI-ATRP

The versatility of SI-ATRP as a method for grafting polymer brushes from the selected surface arises from the ability to precisely control and modulate the structure and properties of prepared hybrid material.

Control over grafting density is essential for regulation of the number of polymer brushes on the surface. This can be achieved by using a mixture of active and inactive ("dummy") initiators to functionalize the substrate surface. The number of active ATRP initiators, and thus the number of polymer chains on the surface, is varied by controlling the corresponding fraction of active initiators in the mixture. Scheme 10b illustrates this strategy.

Another approach for controlling grafting density is partial removal of tethered initiators from the surface by specific treatment (UV light, temperature, chemical).

The ability to control the chain topology and composition of polymer brushes is a major tool for engineering the structure and properties of the resulting hybrid materials prepared using SI-ATRP. This technique allows the grafting of (co) polymer, block, gradient, and statistical copolymer brushes from the surface of various substrates [33, 34]. The brushes can have different topologies, including linear, branched, hyperbranched, and crosslinked chains [53, 54]. Miktoarm hybrid systems can be created by introducing two different polymer chains to the substrate surface using SI-ATRP [55–57] or SI-ATRP combined with other polymerization techniques [58]. These materials are responsive to solvent change and can be turned into Janus nanoparticles by variation of solvent composition [56].

The polymer brush MWD can be controlled by varying the ratio of activator to deactivator. ATRP allows preparation of polymers with very low dispersity; however, sometimes a broad MWD or even bimodal distribution of polymer brushes is desired [59].

SI-ATRP facilitates preparation of functional polymer brushes. Functional groups can either be an inherent part of the monomer molecule, thus being present along the polymer backbone, or can be introduced to previously prepared polymer chains. Chain-end functional groups can be converted into other functional groups and provide an opportunity for conducting click chemistry to the brush end.

Functional polymer brushes can provide stimuli-responsive properties, as well as providing transport and targeting properties, ion conductivity, etc.

4 Reactions in SI-ATRP

In this section, the basic reactions involved in SI-ATRP are discussed, namely initiation, propagation, termination, transfer, equilibrium, and other reactions. Most of the section is further divided on the basis of the curvature of the substrate.

4.1 Initiation

The surface properties introduced by the grafted layer depend on how long the chains are and how crowded the surface is (i.e., the polymer chain length and its grafting density). Grafted chain length can be easily controlled using ATRP. On the other hand, predicting and tailoring the surface to possess a certain grafting density remains one of the major challenges in SI-ATRP. This is because all of the factors affecting grafting density are not fully understood.

On a flat substrate, the measurement of grafting density is challenging because of the limited amount of grafted polymers. In order to estimate the grafting density, it is either assumed that grafted chains have the same properties as free chains when polymerization is conducted simultaneously in both phases [55, 60–63], or that an accurate relationship between swollen and dry thicknesses of polymer layer is known [64]. For systems having large surface-to-volume ratios (e.g., nanoparticles), polymers can be cleaved from the substrate and characterized to give an estimate of grafting density, after the experiments are conducted.

The polymer grafting density is strongly related to the initiator density, which can be controlled by varying the initiator concentration and immobilization time, or by introducing an inert analog along with the initiator species [65–72]. The inert molecules, or spacers, are usually chosen to have a structure similar to the initiator moieties, but do not possess the transferable group for initiating ATRP. The similar chemical structure of spacer and initiator allows the assumption of similar chemical reactivity with the surface of the substrate. Therefore, the fraction of initiator spacer used during immobilization is generally assumed to be the same as the fraction immobilized on the substrate. However, prediction of how many immobilized initiators grow into polymer chains (i.e., grafting efficiency) still cannot be made.

The terms “grafting efficiency” and “initiation efficiency” are used interchangeably in the literature, mainly referring to how many of the tethered initiator sites successfully grow into polymer chains. There are two ways to calculate the initiation efficiency from experimental data. The first is by directly considering the ratio of the polymer grafting density to the initiator density [73–76]. The second is by comparing the theoretical molecular weight to the molecular weight measured from cleaved polymer chains [77–79]. These two methods should theoretically represent

the same value. Lower initiation efficiency is usually obtained at high initiator density, but increases with reduced initiator density up to the point where the efficiency becomes independent of the initiator density [65–67, 76]. This is because steric hindrance dictates the maximum concentration of polymer chains that can be grafted onto a substrate.

Apart from the initiator density, the types of monomer and initiator can affect initiation efficiency [63, 80, 81]. The type of catalyst could indirectly affect the initiation efficiency, as shown by a study of aqueous SI-ATRP of methyl methacrylate (MMA) [74]. The SI-ATRP system with CuCl as catalyst showed slower polymerization rate but better controllability and higher initiator efficiency than the system with CuBr. The difference in initiation efficiency observed was thought to be caused by the difference in polymerization rate, whereby faster polymerization leads to a decrease in initiator efficiency. In addition, a difference in polymerization rate as a result of a difference in catalyst-to-deactivator ratio has also been shown to affect the resulting grafting density [82]. Solvent type is another factor that could influence the grafting density. When SI-ATRP of OEGMA is conducted in a more polar solvent, the resulting grafting density is lower because of the bulkier tethered polymer coils in that system, which imposed steric hindrance for the other initiation sites [61].

The length and phobicity of the link between the initiator and solid surface can also affect the initiation efficiency, as studied by Green and coworkers for SI-ATRP of MMA and of styrene from silica nanoparticles [74, 75]. In the MMA system, their experimental results showed a monotonous increase in grafting density and initiation efficiency with longer initiator linkers, as a result of the increased hydrophobicity of the longer spacer. On the other hand, the system utilizing styrene as monomer showed little difference between shortest and longest linker, as each led to a similar grafting density of 0.7–0.8 chains/nm^2, with an initiation efficiency of 26–35%. However, the system with the middle-length link resulted in a much lower grafting density of 0.2 chains/nm^2, with initiation efficiency around 10%. This difference was postulated to be caused by conformational change, in which the Br end group is hidden in the case of middle-length linker. Comparison of the initiation efficiency between the two studies is shown in Fig. 1.

Surface curvature plays an important role in determining initiation efficiency. The initiation efficiency of SI-ATRP from a flat substrate has been estimated to be around 10% [83–85]. On the other hand, the initiation efficiency that could be obtained from a convex substrate is close to, or even more than, 30% [73–76, 79, 86]. Even higher initiation efficiency values of approximately 80% for particles have also been reported in several studies [77, 78, 87]. In particle systems, some studies have reported a constant increase in initiation efficiency with time [73, 75], whereas others reported it to increase as polymerization progresses to higher conversion [77, 78, 86]. This again shows the uncertainty in predicting initiation efficiency.

Some studies have reported an initiation efficiency of 3–8.5% for concave substrates within ordered mesoporous silica nanoparticles, with mesopore diameter ranging from 1.8 to 2.3 nm [88, 89]. Another study reported 22–37% initiation efficiency when SI-ATRP was conducted in ordered mesoporous silica with 15 nm

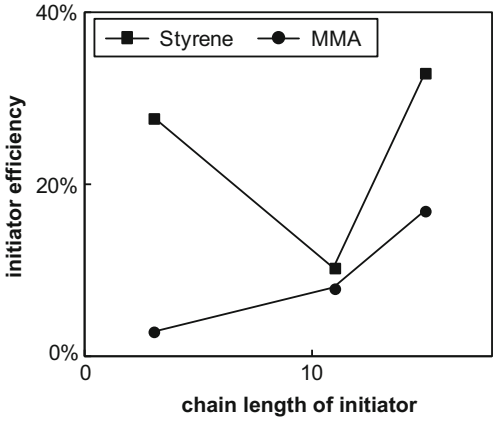

Fig. 1 Effect of initiator spacer length on the initiation efficiency of SI-ATRP of styrene and MMA with CuBr. Detailed experimental conditions can be found in the original publications [74, 75]

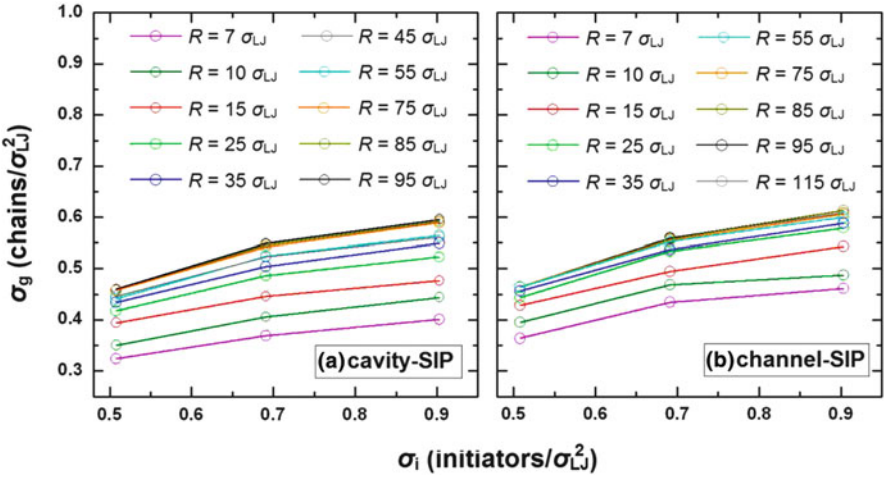

Fig. 2 Effect of confinement on grafting efficiency (σ_g/σ_i), as simulated for surface-initiated polymerization within a spherical cavity or channel with various curvatures; R radius of the cavity. Reprinted with permission from Liu et al. [90]

cylindrical pores [52]. These experimental results point to the conclusion that concave systems, with more severe confinement effects, exhibit lower initiation efficiency. This comparison might of course be influenced by the other factors mentioned above, because they are collected from experiments conducted under different conditions. However, similar findings have been reported in a simulation study of grafting from concave substrate with a "perfectly living" polymerization [90]. As shown in Fig. 2, the simulation results predicted lower grafting density, σ_g, in systems with higher curvature (smaller R), for the same initiator density, σ_i.

It should be noted that in an experimental setting, the dependence of initiator density on the curvature and the influence of termination reactions may further complicate the actual result.

4.2 Propagation

Despite the numerous studies conducted using SI-ATRP, there are several fundamental points that still cannot be definitively answered. For example, what causes the grafted layer to stop growing, even when there is an abundance of monomer in the solution phase? Another fundamental question is related to the validity of assuming grafted and free chains to have comparable properties [68, 91–93]. This assumption is especially important as it is commonly made for graft polymerization on flat substrates, because it allows estimation of the grafting density of the polymer chains even when the amount of polymer collected from flat substrates is not enough for further characterization.

On the other hand, nanoparticle systems have a much larger surface-to-volume ratio than flat systems, allowing a sufficient amount of polymer to be collected for further characterization. Therefore, the assumption can be experimentally verified for these systems. As a matter of fact, much of the data on polymers obtained from SI-ATRP conducted on particle systems show an excellent agreement with the properties of polymers formed in the solution phase [36]. However, this does not guarantee the same trend for polymers grown from flat substrates, because the degree of confinement on polymer chains grown from a convex substrate is less severe than that on a flat substrate. Owing to its positive curvature, polymers grown on convex substrates experience less and less confinement as the chain grows longer and the initiation site is farther away from the surface.

In SI-ATRP from a flat surface, one end of each individual polymer chain is fixed onto a substrate. This forces the polymer chains to grow in close proximity to one another, creating crowding of polymer chains and forcing them to assume a chain-extended brush conformation. The brush conformation is evident from the greater thickness of the grafted polymer layer on a flat substrate than the radius of gyration of the free polymer. The calculation of grafting density shows that each polymer chain occupies a smaller projected area than that predicted by its radius of gyration, further confirming the chain-extended brush conformation.

The steric crowding of polymer chains gives rise to unique properties not seen in grafted polymers with lower grafting density [36, 94]. However, the crowding of surface polymer chains can also lead to starvation of monomer, or earlier formation of a glassy state, which in turn hinders the propagation of additional surface chains. Moreover, some of the surface chains could have their active ends buried inside the dense polymer layer, thereby reducing the available monomer concentration for that radical to propagate. This is one of the two theories often used to explain many experimental trends in the literature, often referred to as the “school of propagation” because of the decrease in propagation rate. The other school of thought, referred to

as the "school of termination," is discussed in Sect.4.3. A recent publication has collected experiment data and compared predictions based on these two schools of thought [95]. The result is inconclusive, as no model can fully explain the various contradicting experimental trends reported in the literature.

Based on the reduced rate of propagation, one could explain the slowing down of the growth rate for grafted chains at negligible monomer conversion. This school of thought could also shed light on when the assumption of equal properties of free and grafted chains can be considered valid. As a result of the difference in the availability of monomer for the chains solution and for the tethered surface chains, the chain length and dispersity of the two polymer populations may not be comparable. The reduction in the concentration of available monomers for the grafted chains is expected to result in chains that are shorter than the free chains in solution.

Recent simulation studies based on the understanding of the school of propagation have shown that the assumption of equal properties of grafted and free polymers is often invalid in a perfectly living polymerization [92, 93]. Simulation results show that the grafted polymers are always shorter and have broader distribution than their solution counterparts when polymerization is conducted simultaneously from a surface and in solution. The difference depends on the fraction of polymers present as grafted chains, η, and on the grafting density, σ, as shown by Fig. 3. Higher grafting density leads to more confinement and reduced propagation rate as a result of monomer limitations, resulting in shorter grafted chains. On the other hand, a lower fraction of congested surface chains leads to less difference in properties between surface and free chains. Therefore, the assumption of surface chains having similar properties to free chains is true only when the surface chains exhibit low grafting density, which is not usually the case in experimental settings. However, it should be noted that some experimental studies of SI-ATRP on flat surfaces have reported controlled growth to a very thick polymer brush, for example, 700 nm of poly(hydroxyethyl methacrylate) (PHEMA) brush on a gold surface [96] and 700 nm of poly(dimethylaminoethyl methacrylate) (PDMAEMA) on a silicon surface [97].

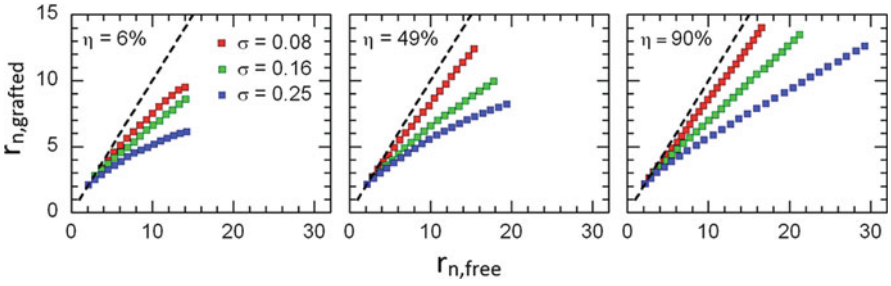

Fig. 3 Model predictions of the chain length of grafted and free polymers in simultaneous surface-initiated polymerization with various grafting densities (σ) and fractions of grafted polymer (η). Reprinted with permission from Turgman-Cohen and Genzer [93]

For systems with concave substrates, the effect of confinement is expected to be even more severe than that for flat substrates. A theoretical study based on molecular dynamics simulations has systematically investigated surface-initiated living polymerization on concave substrates for polymerization occurring strictly on the surface [90]. The simulation results verified the confinement effect on the grafted polymer: shorter chains are obtained in systems with higher degrees of confinement (i.e., smaller surface radius). However, the results are counter-intuitive for the dispersity, where the resulting grafted polymers have narrower distribution with increasing confinement for the same amount of reaction time or at the same monomer conversion. This trend is attributed to the slower polymerization rate in a more confined system, which leads to more uniform growth. It should be noted that the simulation was conducted in the absence of termination reactions, which could significantly affect the resulting dispersity in an experimental setting.

4.3 Termination

Termination is unavoidable in ATRP systems because of the very nature of radicals. Termination in SI-ATRP is highly dependent on the geometry of the substrates. For example, the confined environment of concave substrate leads to closer proximity of polymer chains, which could lead to higher possibility of termination. On flat or convex substrates, the termination could occur via multiple modes. The modes of termination and experimental data supporting the role of termination in kinetics of SI-ATRP are discussed in the following sections.

4.3.1 Termination on Flat Substrates

The termination of living chains during SI-ATRP could offer an explanation for some of the experimentally observed phenomena. For example, termination provides plausible explanation for the experimentally observed decrease in the growth rate of the grafted polymer layer, even when no significant monomer depletion is expected in the bulk contacting solution. This experimental trend has been repeatedly reported in the literature for various types of substrates and monomers [60, 98–100], and has also been supported by an experimentally measured decrease in the concentration of halide groups on the surface [101].

On flat substrates, the possible termination modes depend on the polymerization locus. For SI-ATRP accompanied by simultaneous polymerization in the contacting solution, termination could occur between two surface radicals, two solution radicals, or between a surface and a solution radical. On the other hand, the termination could only occur between two surface radicals for surface-confined SI-ATRP. These possible termination modes are illustrated in Fig. 4.

Termination modes between two solution radicals and between solution and surface radicals are easily imaginable, because at least one of the participants is a mobile free chain. On the other hand, it is harder to picture how two randomly

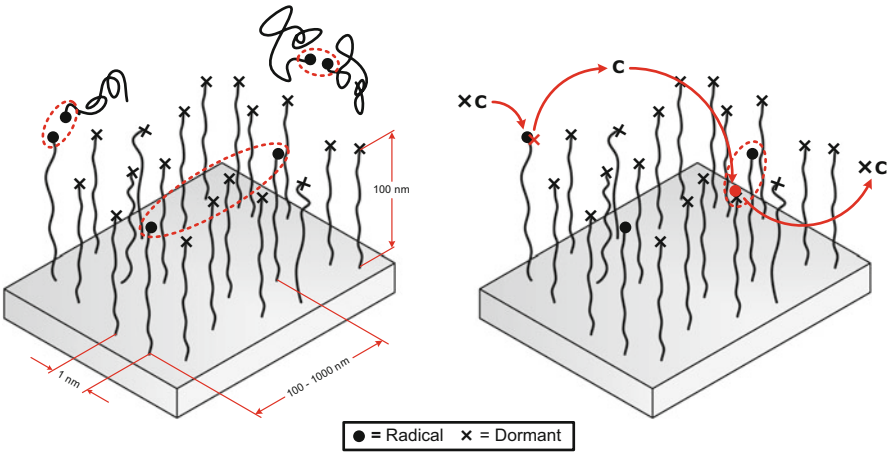

Fig. 4 *Left*: Possible termination modes involved in SI-ATRP on a flat substrate. The estimated distances shown are calculated based on the assumption of high grafting density (1 chain/nm^2), a typical ratio of radical to dormant chains in ATRP ([P$^\bullet$]/[PX] = 10^{-4} to 10^{-6}), and typical brush thickness of 100 nm. *Right*: Migration of surface radicals through activation/deactivation in SI-ATRP promotes termination between surface radicals. Reprinted with permission from Zhou et al. [102]

formed radicals that are fixed to a substrate can reach each other to undergo termination, especially if they are located far from one another. As discussed in the section on propagation (Sect. 4.2), with one end of the polymer chain fixed onto a substrate, the polymer chain cannot move as freely as chains in solution, even though the local concentration of polymer chains is much higher as a result of crowding. Only a very small portion of the chains have active ends at any instant, with most of the chains being capped and dormant. In fact, as demonstrated by Zhou et al., estimation of the distance between radicals on a highly grafted flat substrate indicates that termination between two surface radicals is highly improbable, as denoted in Fig. 4a [102]. It is hard to picture how two surface-constrained radicals can reach each other for termination to occur.

Gao and colleagues proposed a mechanism by which two radical centers that are originally present on surface chains that are far apart could have a high probability of "hopping" to other fixed chains on the substrate [91, 102]. Although the chains do not move because of their attachment to the surface, the active (radical) ends could move as a result of the activation/deactivation involved in the basic ATRP mechanism. Faster migration of active centers from one chain to another, resulting from more frequent activation/deactivation of surface chains, could increase the probability of two radicals being adjacent to one another, as illustrated in Fig. 4b. Therefore, the termination rate is proposed to be proportional to the migration rate, which in turn depends on the rate of activation/deactivation, as shown by Eq. (1) [102].

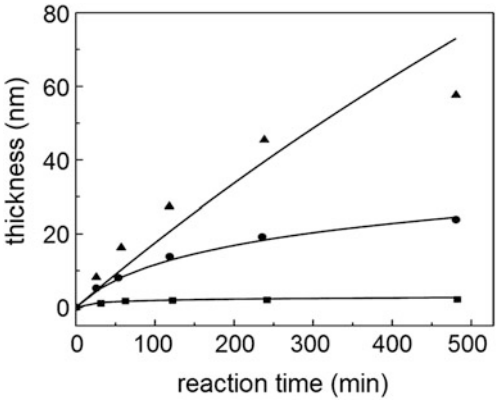

Fig. 5 Growth kinetics of grafted polymer for different catalyst concentrations in SI-ATRP of methyl acrylate (MA) from gold substrate, with [MA] = 2 M and [$CuBr_2$/Me6TREN]/[CuCl/Me_6TREN] = 0.3. *Lines* show the predicted result from the model. *Data points* were experimentally obtained: *squares* 40 mM, *circles* 2 mM, *triangles* 0.1 mM [102, 103]

$$k_t \propto \text{migration rate} \propto [C]_{sol} \tag{1}$$

For SI-ATRP, a constant ratio of catalyst to deactivator is supposed to imply a constant polymerization rate. This is because only a small amount of polymer chains are present on the surface and therefore do not affect the catalyst-to-deactivator ratio throughout the polymerization medium. However, experimental data have shown that an increase in catalyst concentration can result in a faster leveling-off of the growth rate [103]. This concept of migration-assisted termination has been used to explain the experimental data, where a decrease in growth rate of surface chains is observed with increasing catalyst concentration at a constant ratio of catalyst to deactivator, as shown in Fig. 5.

Another possible explanation for the trend observed in Fig. 5 is the recently proposed mechanism of catalytic radical termination in solution ATRP [104]. The proposed termination mechanism for solution ATRP might also be applicable for SI-ATRP. According to that mechanism, the presence of catalyst can increase the amount of termination, which contributes to the observed decrease in growth rate. Another factor to be considered is the possibility that the resulting grafting density is affected by different concentrations of catalyst. However, as mentioned previously, the grafting density is not known a priori, nor can it be measured accurately for a flat substrate.

The termination rate constant has also been proposed to depend on the grafting density (σ) according to Eq. (2), from comparison of the model-predicted thickness with experimental data [102]. The exponential decrease in termination rate constant (k_t) as grafting density increases could be a result of conformational change of the polymer chains.

$$k_t \propto \exp(-\gamma\sigma) \tag{2}$$

Based on the school of termination philosophy, two expressions, Eqs. (3) and (4), have been developed by two different groups to predict the thickness growth profile [101, 102]. These two equations were derived from kinetic equations using

quasi-steady state assumption (QSSA) $k_{act}[PX][C] = k_{deact}[P^{\bullet}][XC]$, and are applicable for cases with negligible conversion. The first group applied QSSA to the mass balance of radicals to obtain an expression for the dry grafted layer thickness, δ, as shown in Eq. (3). On the other hand, the second expression, shown by Eq. (4), was obtained by applying QSSA to the balance of dead chains. Both equations predict the growth rate of the grafted layer thickness to decrease with polymerization time, which offers an explanation for the tapering off observed in the growth kinetics of the grafted layer in experiments.

$$\delta \propto \frac{k_p[M]_0[P^{\bullet}]_0 t}{1 + k_t[P^{\bullet}]_0 t} \tag{3}$$

$$\delta \propto \ln\left(1 + \sigma k_t \left(\frac{k_a[C]}{k_d[XC]}\right)^2 t\right) \tag{4}$$

Although data is scarce, some studies have reported the properties of grafted chains formed by SI-ATRP after cleaving the polymer brush grown on large or multiple planar substrates [65, 68, 83, 105–107]. Unfortunately, such a comparison of grafted chain properties with those of free polymers is very limited, because some of these studies conducted polymerization strictly on the surface [65, 83, 107]. Other studies have reported that collected grafted chains are longer than the free chains produced during simultaneous polymerization [68, 105, 106]. Similar findings have also been reported when surface-initiated nitroxide-mediated polymerization was employed instead of SI-ATRP [108, 109]. A different trend was reported by Yamago et al., who found free and grafted chains to possess similar properties when using surface-initiated organotellurium-mediated living radical polymerization (SI-TERP) [110].

One way to confirm negligible termination has been reported by Kang et al. [107]. The authors conducted a SI-ATRP of styrene on a silicon wafer from a photo-cleavable initiator. The molecular weight of the cleaved polymers was used to calculate the grafting density. For their polystyrene system, which mainly terminates via coupling, constant grafting density implies negligible termination. It should be noted that this method is not valid for other monomers that terminate via disproportionation, since disproportionation would not affect the grafting density value calculated using this method.

4.3.2 Termination on Nanoparticles

In SI-ATRP involving nanoparticles, there are two possible modes for termination between two surface radicals: interparticle and intraparticle termination. Intraparticle termination is basically similar to termination between two surface radicals observed on flat substrates, with the additional limitation of a curvature effect. On the other hand, interparticle termination occurs between chains that are

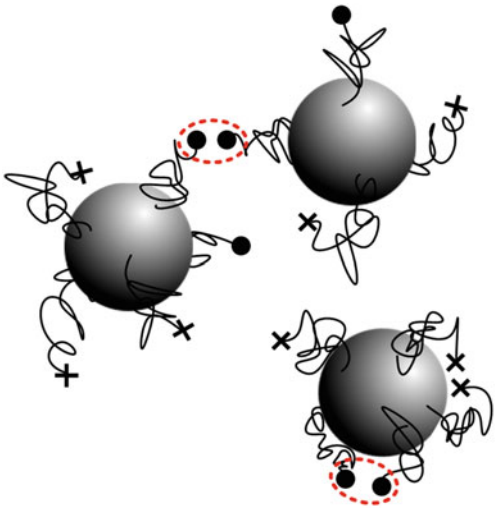

Fig. 6 Interparticle and intraparticle termination modes between two surface radicals in SI-ATRP on nanoparticles

fixed on two different nanoparticles. The termination modes in such a particle system are illustrated in Fig. 6.

A problem that often arises in conducting SI-ATRP on particles is macroscopic gelation, which occurs as a result of interparticle termination via coupling or combination. This can result in an increase in viscosity, leading to diffusion-controlled reactions and loss of polymerization control. The large number of initiation sites on one particle makes it faster for the system to gel as compared with a solution polymerization system. By assuming approximately 1,600 initiation sites per particle, the gelation point can be estimated using Flory's gelation theory as occurring when only 0.125% of the chains undergo interparticle coupling termination [87]. Therefore, macroscopic gelation has been reported even when no bimodality is reported in the MWD of the cleaved grafted chains [77].

Several ways have been proposed for reducing the macroscopic gelation, including using a dilute concentration of particles, or stopping the reaction at low monomer conversion [77, 78, 86]. Free initiator in the solution is also often added to the reaction to form free polymers and prevent network formation [111, 112]. However, both of these methods can increase the cost of synthesizing pure polymer-grafted nanoparticles. Bombalski et al. have shown that macroscopic gelation can be avoided by conducting SI-ATRP in a miniemulsion system as a result of radical compartmentalization, as illustrated in Fig. 7 [87].

Another strategy that is effective for avoiding macroscopic gelation is conducting the polymerization in a high pressure system [76]. When SI-ATRP is conducted under high pressure the polymerization occurs with an increase in propagation rate, whereas the termination rate is suppressed. This leads to a faster polymerization with better living characteristics. Successful synthesis of PMMA grafted chains, with molecular weight above 1 million and low dispersity (<1.3), on silica nanoparticles has been reported using miniemulsion AGET-ATRP in a vessel

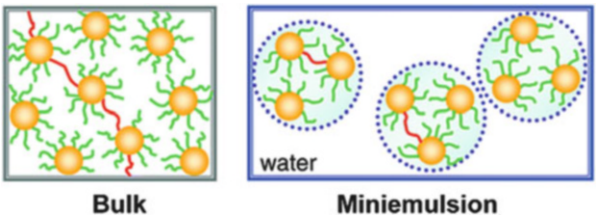

Fig. 7 Interparticle coupling in SI-ATRP on nanoparticles for bulk and miniemulsion systems. The compartmentalization of particles in a miniemulsion prevents macroscopic gelation from occurring. Reprinted with permission from Bombalski et al. [87]

pressurized to 6 kbar [76]. The livingness of the tethered chains, or retention of high chain-end functionality, was confirmed by conducting SI-ATRP of methyl acrylate using the PMMA-grafted nanoparticles as surface initiator.

Chakkalakal et al. have observed bimodality in the MWD of grafted polymer on silica nanoparticles at higher conversion (above 25%) [86]. However, the bimodal distribution was attributed to intraparticle coupling and/or to the coupling termination between surface and solution radicals. The termination occurring via interparticle coupling was considered negligible in their study, based on dynamic light scattering (DLS) results. They also observed that more termination occurred for smaller nanoparticles than for larger particles, as suggested by earlier broadening and bimodality of the MWD.

4.3.3 Termination on Concave Substrates

In the case of systems involving concave substrates, such as porous particles or cylindrical channels, the confinement effect is expected to be much more severe than that for flat substrates. In addition to the obvious mass transport issue that results from a more confined space, the probability of termination could also increase. Therefore, a less living and less controlled polymerization is expected in systems involving concave substrates.

Multiple studies have reported a population of shorter grafted polymer chains with broader distribution in comparison with free/solution polymer chains [88, 89, 113]. Gorman et al. conducted SI-ATRP from a silicon wafer, porous silicon, and anodically etched aluminum oxide. The results were compared with those of ATRP conducted in solution under similar conditions. The grafted polymer chains from a flat substrate were shown to be shorter than the free chains formed in the parallel solution polymerization. The polymers obtained from concave substrates have an even lower molecular weight and broader distribution.

The Charleux group has conducted several studies of SI-ATRP in mesoporous silica nanoparticles [88, 89]. Instead of conducting parallel polymerizations, they conducted simultaneous polymerization in solution and from the surface. Their findings were similar to those of Gorman et al., showing grafted chains to have

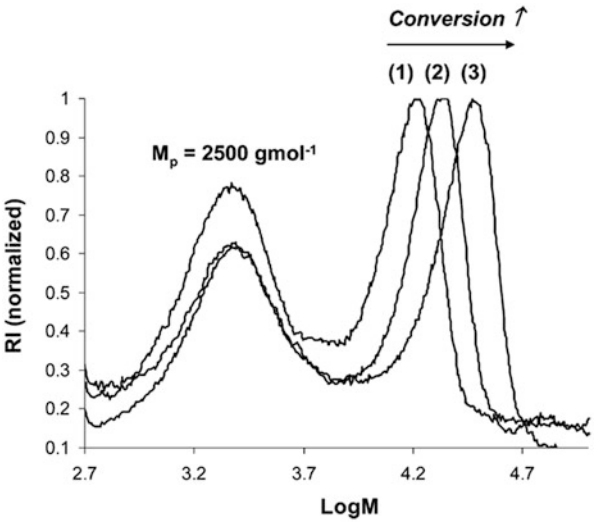

Fig. 8 Molecular weight distributions of grafted chains for SI-ATRP of MMA from a concave substrate. Detailed experimental conditions are provided in the original literature. $M_{p,l}$ indicates the molar mass at the peak for the living chains. (*1*) 50%, $M_{p,l} = 16{,}320$ g/mol; (*2*) 62%, $M_{p,l} = 21{,}880$ g/mol; (*3*) 91%, $M_{p,l} = 30{,}020$ g/mol. The lower peak ($M_p = 2500$ g/mol) indicates the presence of dead chains. Reprinted with permission from Pasetto et al. [89]

significantly lower molecular weight with broader distribution than the chains formed in solution. Moreover, for some of the experiments, the grafted chains were shown to display multimodal distribution, as characterized using gel permeation chromatography (GPC) (see Fig. 8). The lower molecular weight peak observed in the distribution did not shift, even at higher conversion, indicating the presence of dead chains. From this GPC curve, they estimated that approximately 50% of the chains had been terminated. Characterization of the grafted chains using mass spectroscopy also provided proof that some of the grafted chains had undergone termination by disproportionation.

Simulation of polymerization from a concave substrate could prove to be a challenging task because of the complexity of the system. However, Liu et al. used coarse-grained molecular dynamic simulation to investigate the effect of curvature on polymer growth and dispersity [90]. Unfortunately, the polymerization was considered to be a perfectly living polymerization (i.e., in the absence of termination and other side reactions), thus it does not help in elucidating the role of termination in SI-ATRP.

4.4 Exchange

At the beginning of normal ATRP, only catalyst and initiator are present in the solution. As the polymerization progresses, some of the chains undergo bimolecular termination, resulting in accumulation of the deactivator. The accumulation of deactivator, termed the persistent radical effect [114], is important in reaching an equilibrium between dormant and active chains. Indeed, control in ATRP systems relies on creating an equilibrium between dormant and active chains, as they

reversibly react with catalyst and deactivator, respectively. The broadness of the MWD (i.e., dispersity) is often used as an indicator of how controlled the polymerization is. For cases with negligible termination and high degrees of polymerization, the dispersity ($Đ$) of polymer chains synthesized through ATRP as a function of conversion (conv) follows Eq. (5), with the polymerization rate (R_p) shown by Eq. (6) [115, 116]. Based on Eq. (5), in order to obtain a high degree of control over the polymerization (low dispersity), there must be a sufficient concentration of deactivator (XC) present in the system. However, it is clear from Eq. (6) that there is a trade-off between the polymerization rate and degree of control:

$$Đ = 1 + \frac{k_p[\mathrm{PX}]_0}{k_d[\mathrm{XC}]}\left(\frac{2}{\mathrm{conv}} - 1\right) \tag{5}$$

$$R_p = k_p[\mathrm{M}][\mathrm{PX}]\left(\frac{k_a[\mathrm{C}]}{k_d[\mathrm{XC}]}\right) \tag{6}$$

In SI-ATRP from a flat substrate, the amount of initiator present on the surface is not nearly enough to provide sufficient accumulation of deactivator in the contacting system. This leads to an uncontrolled polymerization. Two procedures are commonly used to mitigate the uncontrolled SI-ATRP from flat substrates: the addition of free initiator [117] and the addition of deactivator [99]. The presence of free initiator provides solution chains that do terminate and, hence, accumulate enough deactivator to control the polymerization. For this reason, the free initiator is also often referred to as "sacrificial" initiator. Other than for maintaining control of the polymerization process, free initiator is also added to systems with flat substrates to provide an estimate of the properties of grafted chains. The validity of this estimation has been discussed in previous sections. On the other hand, the addition of deactivator can provide enough deactivator to control the polymerization without requiring surface chains to undergo termination. However, the addition of too much extra deactivator could result in retardation of the polymerization rate (Eq. 6).

One of the main differences between SI-ATRP from flat substrates involving addition of free initiator and addition of extra deactivator lies in the formation of free polymer. The free chains in solution greatly affect the polymerization kinetics of both chain populations. Because of the small amount of surface chains, the monomer conversion in SI-ATRP with extra deactivator is negligible. However, free initiator in solution can consume significant amounts of monomer and cause monomer depletion. For this reason, a thicker polymer layer is usually obtained when the polymerization is conducted using SI-ATRP with added deactivator [118, 119]. Figure 9 shows a comparison between the growth profiles obtained from these two methods.

As noted above, in SI-ATRP with addition of deactivator, the consumption of monomer is negligible; therefore, the growth profile of the polymer layer with time is expected to be linear in an ideal case (no crowding or termination effects). On the other hand, monomer conversion in SI-ATRP with free initiator is not negligible.

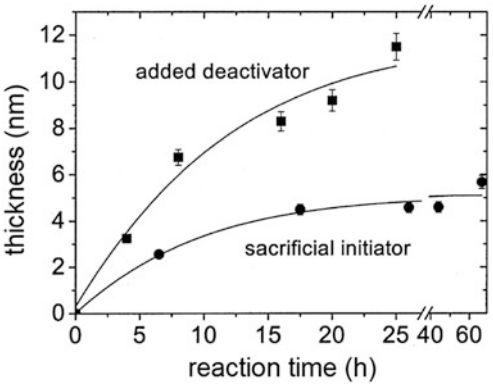

Fig. 9 Growth profiles of grafted polystyrene on a silicon wafer with addition of sacrificial initiator (*circles*) or deactivator (*squares*). Reprinted with permission from Jeyaprakash et al. [118]

Hence, the growth profile of the polymer layer with conversion is expected to be linear in an ideal case, where the polymerization rates of solution and surface chains are the same. Deviation from linearity in the growth profile with time or with conversion (added deactivator or sacrificial initiator, respectively) could be explained by applying the philosophy of either the school of propagation or school of termination, as previously discussed.

In particle systems, as a result of the large surface-to-volume ratio, a sufficient number of surface initiators might be present to generate the required concentration of deactivator in the solution. However, free initiator and/or excess deactivator are still often added to this system. Free initiator is often added for SI-ATRP of particles for multiple reasons. One reason is to provide better control over the polymerization, another is to prevent macroscopic gelation resulting from interparticle coupling.

The type of catalyst has also been shown to affect the equilibrium in SI-ATRP. Huang et al. compared the use of CuBr with CuCl for SI-ATRP of MMA from silica nanoparticles [74]. The grafted chains on the nanoparticles were cleaved and their dispersity used as an indicator of polymerization controllability. They found that CuBr resulted in faster polymerization but produced a less uniform polymer layer and higher dispersity. Several researchers have attributed poorer control to differences in the local concentrations of catalyst and deactivator, which can affect the equilibrium experienced by the surface chains. According to experimental results from Behling et al., surface-initiated polymerization occurs faster than solution polymerization [68]. The difference in polymerization rate was attributed to deviation of the ratio of local concentrations of catalyst and deactivator available to the surface chains, as shown in Fig. 10. They postulated that in the "viscous front" (shaded area in Fig. 10) the local concentration of catalyst (C) is higher than that in the bulk, whereas the opposite is true for the local concentration of deactivator (XC). Because of the reduced deactivation rate in the viscous front, the surface radical concentration increases, which results in a faster propagation rate for surface-tethered chains than for chains present in the contacting solution.

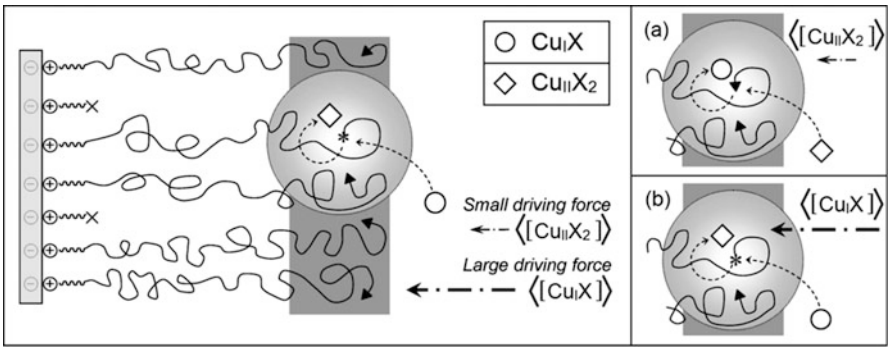

Fig. 10 The growing viscous front for SI-ATRP postulated by Behling et al. [68]. The local concentration of catalyst in the *shaded area* is higher than that in the bulk solution, whereas the local concentration of deactivator is lower than that in the bulk. (**a**) conversion of catalyst (◇) to deactivator (○) (**b**) conversion of deactivator to catalyst. Reproduced with permission from Behling et al. [68]

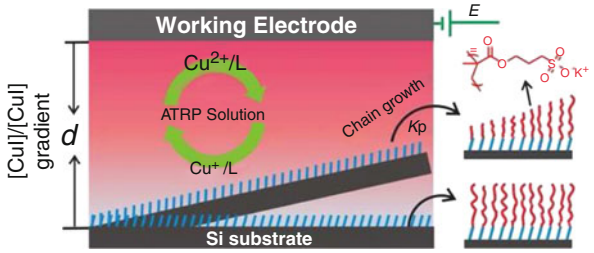

Fig. 11 Generation of a gradient of catalyst-to-deactivator concentration ratio induced by adjusting the distance between the surface and the electrode, resulting in a gradient in the thickness of the grafted polymer layer. Reproduced with permission from Li et al. [120]

Li et al. investigated the effect of catalyst-to-deactivator concentration ratio on the growth of a polymer layer on a flat substrate [120]. They induced a gradient of the concentration ratio of activator to deactivator by using electrochemically mediated ATRP (eATRP) and tilting the substrate toward the electrode (as illustrated in Fig. 11). In eATRP, the catalyst is regenerated electrochemically from the deactivator [20]. By adjusting the distance, the surface closer to the electrode experiences a higher concentration ratio of catalyst to deactivator, thereby experiencing a faster polymerization, as indicated by the thickness gradient in the grafted polymer layer.

4.5 Transfer

Several studies have investigated the importance of chain transfer reactions in solution ATRP. The importance of chain transfer to ligand was reported by

Matyjaszewski and coworkers for ATRP of *n*-butyl acrylate [121]. This chain transfer reaction was proposed to be the cause of the deviation observed in the first-order kinetic plot when excess ligand (pentamethyldiethylenetriamine, PMDETA) was used in the polymerization recipe. The mechanism of the chain transfer reaction to PMDETA was further investigated by Sharma et al. [122]. Chain transfer to PMDETA has been proposed to induce a higher degree of control for SI-ATRP systems containing acrylate monomers [123]. This was achieved by conducting the SI-ATRP at a higher ratio of ligand to catalyst, [PMDETA]/[CuBr] = 3, in the absence of excess deactivator and free initiator. Other SI-ATRP studies have also used similar polymerization recipes, with elevated levels of PMDETA for a *N*-isopropylacrylamide (NIPAM) system showing great success [64, 124–126].

The extent of chain transfer reactions in SI-ATRP could affect the polymerization kinetics and the resulting grafting density of polymers. However, further studies need to be conducted in order to fully understand the role of chain transfer reactions in the SI-ATRP mechanism.

4.6 Other Side Reactions

For some monomers (e.g., styrene) thermal self-initiation is unavoidable. This results in simultaneous polymerization in solution and on the surface, even in the absence of added free ATRP initiator. The presence of free polymers might not be desirable, as they can alter the properties of the bulk nanoparticle system, hence requiring further separation steps. Moreover, the presence of free polymer chains affects the characterization of grafted polymer properties, including the estimation of grafting density, potentially generating large errors [79, 127]. Therefore, when seeking to determine the properties of a hybrid system, the presence of free polymer chains must be quantified to account for their effect on the system, or to ensure that they have been fully separated from the system. Figure 12 illustrates how even the presence of a small amount of free polymer chains can bridge the voids between grafted nanoparticles at certain particle size/graft chain molecular weight, thereby altering the material properties.

In nanoparticle systems, the separation of free polymers and grafted nanoparticles can be tricky and time-consuming. Therefore, it is necessary to understand factors affecting thermal self-initiation in order to control its rate. Tchoul and coworkers used size exclusion chromatography (SEC) to quantify the amount of free polystyrene chains formed during the SI-ATRP of styrene from nanoparticles (shown in Fig. 13) [79]. They demonstrated the accuracy of using SEC to quantify the small amount of free polymer chains. They have also shown that interparticle distance is greatly affected by the presence of free polymer chains, as indicated by the results of their TEM studies [127]. By quantifying the formation of free polystyrene, they optimized the reaction conditions to suppress the thermal self-initiation of styrene. Using the dependence of thermal self-initiation rate on

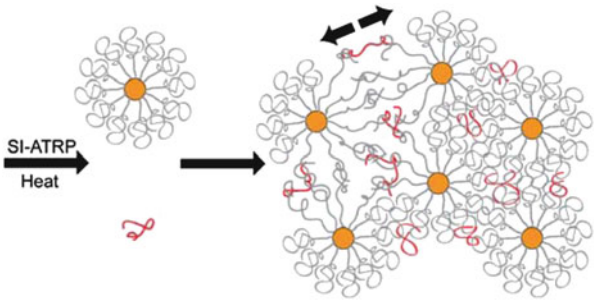

Fig. 12 Presence of free polymer chains in a grafted nanoparticles system. The free chains act as bridges for the grafted nanoparticles to form a network. Reproduced with permission from Hui et al. [127]

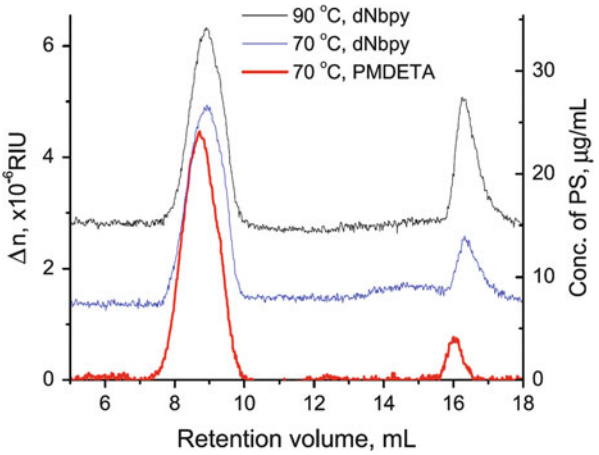

Fig. 13 SEC results for polystyrene grafted from silica nanoparticles with different polymerization recipes. The *concentration axis* on the *right* is only applicable to the peaks at 16–17 mL. Reprinted with permission from Tchoul et al. [79]

time and temperature the authors minimized the rate by using a lower reaction temperature combined with the use of a more active catalyst system [79, 127].

Chakkalakal et al. conducted SI-ATRP of MMA and styrene from silica nanoparticles, and their GPC curves showed a bimodality in the MWD of grafted polystyrene on silica nanoparticles at high conversion [86]. The SI-ATRP was conducted at an elevated temperature, with free polymers formed by thermal self-initiation of styrene at 90°C. Even though there was significant bimolecular termination occurring via a coupling mechanism, as indicated by the bimodal MWD, the DLS result did not show evidence of interparticle termination. Therefore, the coupling could occur only by intraparticle coupling or by coupling of a surface radical with solution radical.

Mu et al. demonstrated the formation of polymer nanocapsules using SI-ATRP to grow a polymer brush from particles, crosslinking of the tethered polymer brush, followed by etching of the particles [128]. Silica nanoparticles can work as a template for the preparation of polymeric nanocapsules. In an extension of this concept, formation of nanonetwork polymers was demonstrated by Matyjaszewski and coworkers, as shown in Fig. 14 [129]. In addition to forming a nanocapsule by etching the silica particles after crosslinking, the authors also showed that a

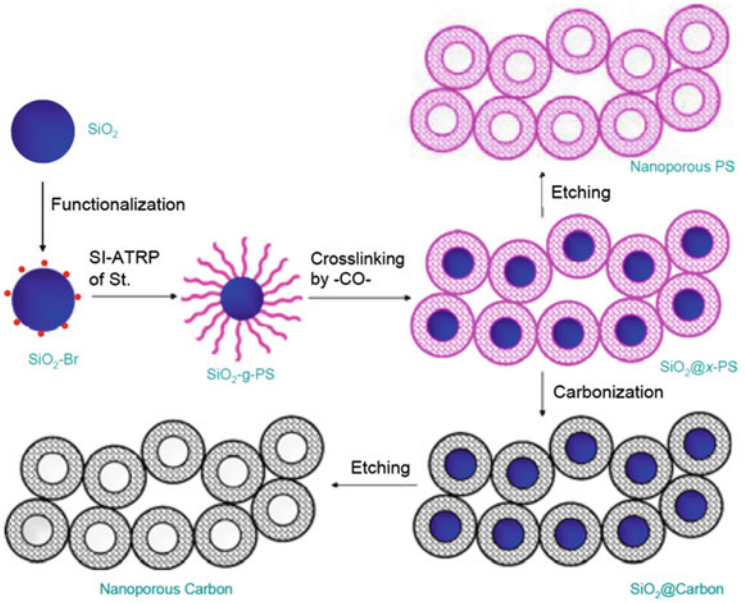

Fig. 14 Formation of nanonetwork polymers and carbon materials using SI-ATRP from silica nanoparticles [129]

nanonetwork of carbon materials can be obtained by carbonizing the polymer prior to etching the core of the nanoparticles. The resulting material was a core–shell system with a mesoporous core from the silica template and a microporous shell from the intraparticle crosslinking of the tethered carbon precursor polymer brush.

5 Materials

Grafting of polymers on material substrates to impart various surface properties is advantageous if one desires to govern the interactions between the material and its surroundings, without compromising its bulk properties. Different surface properties can be obtained, depending on the type of polymers grafted from the surface. For example, regarding the increasing trend to use stimuli-responsive polymers, responsive and switchable surface properties can be obtained by selective grafting of a polymer brush from a surface. The properties imparted by the grafted polymer layer depend not only on the type of polymer chemistry, but also on the uniformity, grafting density, and thickness of the grafted polymer layer. A major advantage of using SI-ATRP for grafting polymers from a surface is that it allows preparation of more complex polymer chain microstructures and topologies and better control over polymer brush properties, which means that more precise surface properties can be generated. Moreover, the grafting density that can be obtained by SI-ATRP

is higher than attained by the grafting-to method or by free radical polymerization. It has been shown that grafted polymers with moderate to high grafting densities give different properties from those observed for low grafting density [130, 131].

5.1 Flat Substrates

SI-ATRP can be used to synthesize complex polymer brush structures that range from block copolymer brushes, to linear chains with gradient composition and gradient molecular weight brushes, to binary brush types, which allows preparation of hybrid substrates with highly tunable and unique properties [55]. Therefore, SI-ATRP is a popular method for the preparation of surfaces for biomedical applications, with numerous papers being published every year on the synthesis of materials having surface properties required for such applications (antifouling, antimicrobial, etc.) [132–138]. For biomaterial applications as such as biosensors, implants, etc., where the material comes in contact with various proteins in a complex biological environment, it must possess antifouling surface properties. The antifouling properties improve the performance of biomaterials by reducing the amount of adsorbed proteins on the surface. These properties can be introduced by grafting biocompatible polymer brushes via SI-ATRP from the surface, for example, by grafting hydrophilic neutral or zwitterionic polymers. The group of Zhu and Brash investigated the biocompatibility of silicon [61, 100, 139–149], gold [150], and polymeric [151–154] surfaces grafted with hydrophilic and zwitterionic polymer brushes. Feng and coworkers from the same group compared the protein resistance of silicon surfaces grafted with poly(2-methacryloyloxyethyl phosphorylcholine) (PMPC) or POEGMA, having various grafting densities and chain lengths [146–149]. They reported lower fibrinogen adsorption and platelet adhesion for surfaces with higher grafting density and longer chain length, but the results were similar for both types of polymer brushes. This result suggests that a water barrier created in the presence of both brushes plays a major role in improving resistance to protein adsorption.

In addition to the antifouling properties, some biomaterials should also possess antimicrobial properties to prevent bacterial infection. The grafted polymer brushes can suppress bacterial growth by reducing bacterial adhesion or by acting as a tethered biocide and killing the bacteria by cellular disruption. The polymers that are used to impart antifouling properties also generally reduce the adhesion of bacteria on the surface to a certain degree. Chang's group grafted a zwitterionic polymer brush onto titanium and stainless steel via SI-ATRP and prepared surfaces with high resistance to cell, bacterial, and protein adhesion [155, 156]. They reported at least 95% reduction in bacterial adhesion on the grafted surfaces compared with reference unmodified surfaces, showing the great potential of poly (sulfobetaine methacrylate) (PSBMA) for the preparation of biocompatible implants. Matyjaszewski's group has demonstrated that the introduction of quaternary ammonium groups into the backbone of polymer brushes can kill bacteria

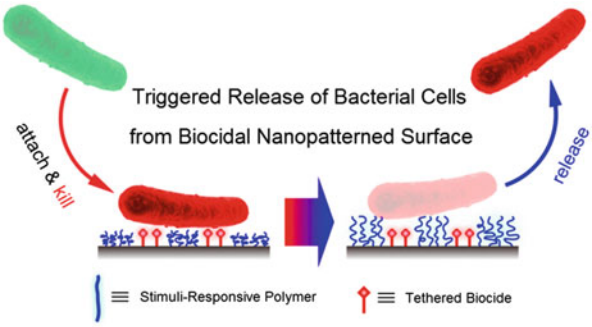

Fig. 15 Self-cleaning, antimicrobial surface prepared by utilizing PNIPAM and a quaternary ammonium salt. Reproduced with permission from Yu et al. [159]

[157, 158]. Using SI-ATRP, they grafted PDMAEMA from glass, filter paper, or a polypropylene slide, followed by quaternization of the tertiary amino groups. The modified surfaces exhibited significant antimicrobial properties. The group also showed that the killing efficiency depends on the polymer brush chain length, with longer chains showing higher killing efficiency. Yu et al. combined a thermo-responsive polymer (PNIPAM) with a quaternary ammonium salt and prepared self-cleaning antimicrobial surfaces, as illustrated in Fig. 15 [159]. The thermally responsive behavior of PNIPAM allowed the surface to expel the dead bacteria when PNIPAM switched to its extended conformation, resulting in self-cleaning properties that could be controlled simply by adjusting the temperature in the contacting environment.

PMPC has also been grafted onto a surface to improve the surface lubrication properties [160–162], because some applications, such as biological surfaces in artificial joints, require extremely low friction properties. Kobayashi et al. studied the friction behavior of PMPC brushes synthesized by SI-ATRP compared with other polyelectrolyte brushes [160, 161]. They found that higher humidity resulted in generation of lower friction properties for the surface, which was attributed to the presence of adsorbed water molecules in the polymer brush. In other words, the lubrication properties induced by polymer brushes depend heavily on the surrounding environment. A similar finding was reported by Nomura et al., who investigated the dependence of lubrication on the swelling characteristics of a polystyrene brush (controlled by the solvent composition), and by Bielecki et al. who studied the tribological properties of surfaces grafted with various alkyl methacrylates [163, 164]. Nomura and coworkers proposed that the lubrication properties of densely grafted polymer brushes followed two mechanisms, namely boundary lubrication and hydrodynamic lubrication.

Grafting of stimuli-responsive polymers broadens the applicability of grafted surfaces. Depending on the polymer grafted, the surface can reversibly switch its properties in response to different stimuli. Kumar et al. grafted various diblock copolymers, with the outer block being a stimuli-responsive polymer, as shown in Fig. 16 [165]. The inner block acted as a reservoir for small molecules, which were released when the outer block assumed a chain-extended conformation after external stimulus was applied. The same research group also grafted a CO_2-responsive polymer, PDEAEMA, onto silicon- and gold-coated substrates [166]. The modified

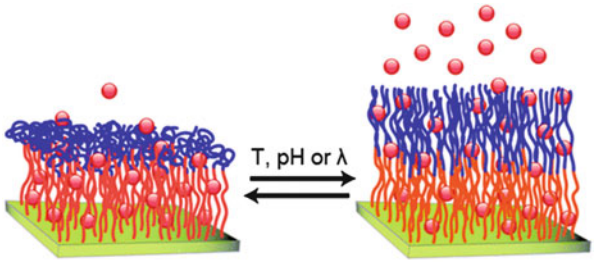

Fig. 16 Diblock copolymers with stimuli-responsive outer block grafted onto a substrate to release dye molecules when an external stimulus (temperature, pH, or light) is applied. Reproduced with permission from Kumar et al. [165]

surfaces underwent reversible adsorption and release of proteins simply by bubbling carbon dioxide into the contacting medium. There are also many studies using thermoresponsive polymers for the preparation of smart biosurfaces. By grafting OEGMA on gold surfaces, Wischerhoff et al. obtained surfaces with temperature-switchable cell adhesion/antifouling properties [167]. Liu et al. showed how stimuli-responsive polymer brushes of PNIPAM and PDMAEMA could be used to prepare surfaces with switchable adhesive properties and demonstrated how the mobility of water droplets on the surface was controlled by changing the temperature or pH [126].

Another interesting feature that can be introduced to a surface using SI-ATRP is the property of self-healing. Takahara and colleagues demonstrated reversible nanoscale adhesion/separation of two substrates by grafting a polyelectrolyte having a positive charge on one surface and a negative charge on the other using SI-ATRP [168]. The electrostatic attraction between polymer brushes on these two surfaces created a strong adhesion, which could be reversibly released by adding a salt solution. However, adhesion of the two oppositely charged polyelectrolytes released salt into the solution, which affected the resulting adhesion. To counter this problem, the same research group grafted zwitterionic polymer brushes onto both substrates to achieve a similar reversible adhesion/separation feature through dipole–dipole interactions [169]. The adhesion reversibility of the surfaces grafted with zwitterionic polymer brushes was found to be better than that of surfaces with oppositely charged polyelectrolyte brushes. Moreover, the de-bonding reaction was achieved simply by placing the substrate in water at an elevated temperature of 50°C.

SI-ATRP can also be used to modify the surface properties of metals. Several types of acrylic monomers have been grafted on metal surfaces, such as iron, steel, nickel, copper, and stainless steel [170–173]. The grafted surfaces showed significant improvement in corrosion resistances compared with the unmodified surface [171]. Moreover, some researchers have found an iron catalyst to be more efficient than copper in controlling SI-ATRP on these surfaces [171, 172]. SI-ATRP is also an excellent tool for producing patterned polymer brushes by immobilizing the initiator moieties in desired patterns, through methods such as microcontact printing [84], polymer pen lithography [174], and many others [175, 176]. A review by Chen et al. discussed various synthesis methods and applications of patterned polymer brushes [177]. Recent studies of patterned polymer brushes via SI-ATRP have focused on the preparation of large surfaces [174, 176].

5.2 Concave Substrates

SI-ATRP can be employed to graft polymers from porous materials. The thickness of grafted polymer can be precisely controlled, eliminating possible blockage of small pores in membranes or other porous materials. Indeed SI-ATRP has been used to modify the surface of membrane pores for various purposes, such as to impart antifouling properties [178], improve biocompatibility, and/or to introduce surface responsiveness to external stimuli. The use of SI-ATRP also ensures no significant change in the pore size distribution after grafting. In one example, PNIPAM was grafted from ultrafiltration membranes (pore diameter 110 nm) and gave the surface thermoresponsive properties [179]. The pore diameter of the membrane could be changed by changing the temperature to above or below the lower critical solution temperature of PNIPAM. Chen et al. synthesized a membrane that responded to four different stimuli, namely temperature, pH, salt concentration, and type of anion [180]. The multistimuli-responsiveness was achieved by grafting a diblock copolymer brush of PNIPAM and poly(methyl acrylate) (PMA) from the membrane pores using SI-ATRP. By changing the copolymer composition ratio, the gating behavior of the membrane in response to an external stimulus could be altered as desired (see Fig. 17). A recent review by Ran et al. summarized various studies of functionalization of membranes using SI-ATRP [181].

Ordered mesoporous silica nanoparticles have shown significant potential for use as biomedical devices, such as drug delivery carriers [182]. In one example, a thermoresponsive polymer, PNIPAM, was grafted onto porous substrates, which allowed formation of surface-responsive properties in the pores [183]. The conformation change of PNIPAM brushes with temperature was used to initiate the

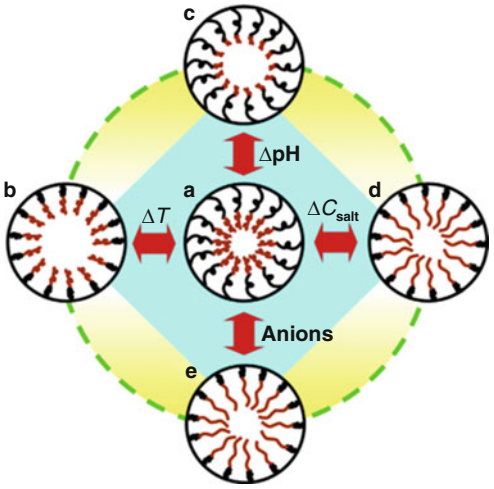

Fig. 17 Quadri-stimuli-responsive properties of PNIPAM-b-poly (methacrylic acid)-grafted gating membrane responding to temperature, anion type, pH, and salt concentration. *Black lines* show the responsive nature of the PNIPAM segment and *red lines* show the responsive nature of the poly(methacrylic acid) segment of the polymer brush. Reproduced with permission from Chen et al. [180]

release of drugs contained inside the pores. Through this approach, drug release can be triggered by various external stimuli, such as temperature and pH.

Shen et al. used SI-ATRP to modify the surface of a polymeric monolith with grafted PDMAEMA to impart pH and salt-responsive properties. Because of the controlled and living characteristic of SI-ATRP, the surface hydrophobicity could be controlled by varying the polymerization time. The responsive monolithic surface was used to prepare materials for an HPLC column to control the retention of steroids [184]. Filter paper is another popular concave substrate that can be modified using SI-ATRP. As previously mentioned, Matyjaszewski's group used SI-ATRP to graft PDMAEMA onto filter paper, which was subsequently modified to form quaternized ammonium units, which act as a biocidal agent [157]. Jiang's group recently reported the synthesis of a highly sensitive, low fouling, glucose sensor by grafting poly(carboxy betaine methacrylate) (PCBMA) onto cellulose filter paper [185]. As a result of the hydrophilic properties of the polymer brushes, the grafted filter paper exhibited a fast response in detecting the presence of glucose in complex media.

Carbon black is another type of inexpensive material with excellent bulk properties. However, it possesses surface properties that are incompatible with many other materials. Consequently, a suspension of carbon black in a matrix material is often unstable. Modification of carbon black surface via SI-ATRP has been reported by Matyjaszewski's group [186]. The dispersibility of the modified carbon black was significantly improved. In addition, various other functional groups have also been successfully introduced onto the surface.

5.3 Convex Substrates

There are a variety of reasons for surface modification of nanoparticles through grafting including, but not limited to, improving colloidal stability, generating smart properties through the use of stimuli-responsive polymers, and altering the surface properties of a particle for specific applications. The resulting properties depend not only on the grafting density and the average length of the chains grafted from the particles, but also on the uniformity of the polymer layer. These polymer chain properties affect the polymer brush conformations and can be precisely tailored by using SI-ATRP. For example, the dependence of the ordered/disordered formation on the chain length and particle size of nanoparticles has been investigated, as qualitatively shown in Fig. 18 [187]. In addition, the effect of polymer architecture on the final properties, such as mechanical and thermal properties, of the resulting materials has been systematically studied [188, 189]. It is also possible to graft polymer brushes onto nanoparticles to obtain particles with a prespecified average refractive index value, which can be used as fillers [190]. By tuning the refractive index of the final particles, by taking into consideration the refractive index of the inorganic core and the polymer shell along with the thickness of the shell, a core–shell particle can be prepared with a refractive index that matches the

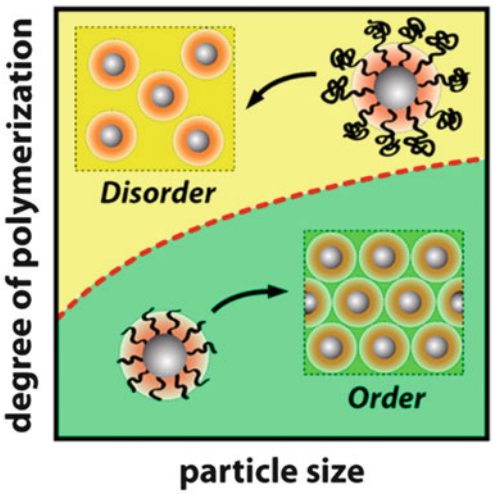

Fig. 18 Dependence of order formation on the degree of polymerization and the particle size. Reproduced with permission from Choi et al. [187]

targeted matrix material and, thus, a transparent nanofilled reinforced composite can be obtained. This allows all the benefits of using nanofillers without compromising the optical quality of the material.

Polymer-coated magnetite nanoparticles are gaining popularity due to their wide applicability. These particles combine the magnetic properties of the core with the functional groups of the polymer brush shell [191]. Bull et al. reported a method for preparation of multigram magnetite nanoparticles using a polymeric surfactant, which was synthesized via ATRP [192]. Another method often utilized to synthesize magnetic nanoparticles with a polymer coating is through surface-initiated polymerization. The use of SI-ATRP to introduce a polymer layer onto these nanoparticles has been investigated for various purposes. Polymer brushes can be introduced to provide better dispersion [193–196]. Another potential application demonstrated for polymer-coated magnetite nanoparticles is for oil–water separation, as shown in Fig. 19 [197]. The negatively charged grafted polymer allows the nanoparticles to absorb water, which can be separated from the oil phase by applying an external magnetic field. The magnetic properties of the original particles are retained in the grafted particles, making it easy to separate the particles from the oil phase.

Dong et al. used SI-ATRP to prepare recyclable antimicrobial substrates from magnetite nanoparticles [198]. They grew PDMAEMA brushes from magnetite nanoparticles, followed by further reaction to form quaternary ammonium groups. The resulting nanoparticles exhibited antimicrobial properties and excellent recyclability as a result of the presence of quaternary ammonium groups and the magnetic properties of the cores. Stark's group proposed a method for producing magnetic inks, which can be used for greener paper recycling processes, via SI-ATRP [194, 199]. The magnetic inks consisted of carbon-coated magnetite nanoparticles, which were grafted with polymer brushes to improve their stability in water. The use of magnetic inks allowed easy de-inking of papers, reducing the

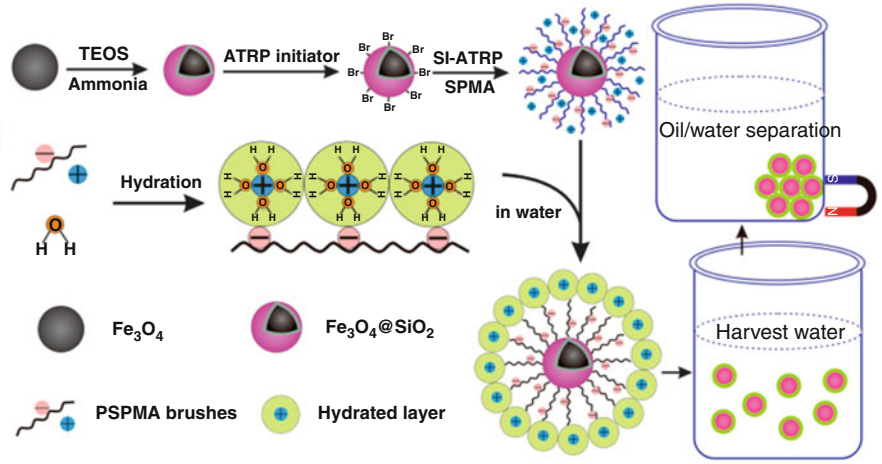

Fig. 19 Zwitterionic polymer brushes on magnetite nanoparticles as a tool for separating oil and water. Reprinted with permission from Liu [197]

use of toxic chemicals needed for bleaching the papers. Moreover, magnetic inks from the recycling process could be recovered for subsequent reuse. Gu et al. prepared magnetic nanoparticles grafted with block copolymer of polyhedral oligomeric silsesquioxanes (POSS) and PMMA using SI-ATRP [196]. These nanoparticles can be used as smart fillers, as their location in the solution can be controlled using a magnetic field, allowing localization of fillers. The localization of fillers is beneficial in minimizing the amount of filler required to achieve the same surface properties. The resulting PMMA film containing these fillers exhibited 30% improvement in the indentation microhardness compared with film without fillers.

Post-grafting modification of nanoparticles allows even more variation in the attainable polymeric architectures. By crosslinking the polymer brushes on nanoparticles after SI-ATRP, polymeric nanocapsules can be obtained by etching the nanoparticles [128]. Carbonization prior to etching allows formation of nanonetwork carbon materials [129]. The polymer brush can also be acidified to form an acidic brush layer, which can be used as a reusable catalyst in the dehydration of fructose [200].

SI-ATRP has also been used to modify the surface of quantum dots in order to improve the dispersibility and stability of these nanoparticles. Farmer and Patten demonstrated the use of SI-ATRP to graft PMMA from CdS/SiO_2 core–shell nanoparticles [201]. A film formed from the resulting grafted nanoparticles exhibited the same luminescence properties as the CdS core, with the inorganic cores uniformly distributed throughout the polymer matrix. Esteves et al. reported grafting of poly(*n*-butyl acrylate) from CdS quantum dots via miniemulsion ATRP [202]. Characterization of the nanocomposites demonstrated an even dispersion of CdS cores in the polymer matrix.

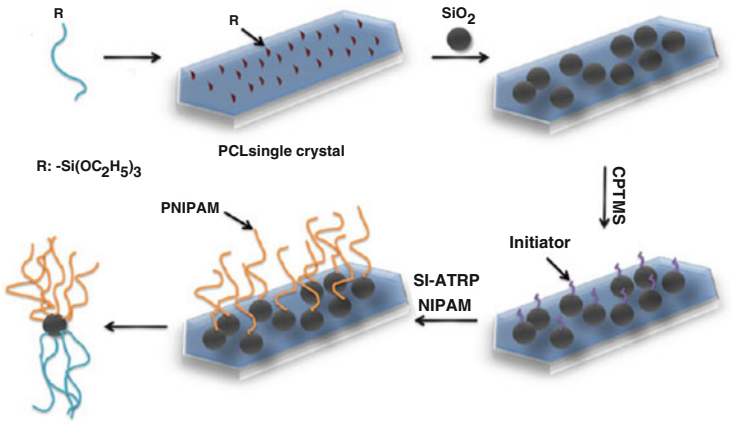

Fig. 20 Synthesis of Janus nanoparticles using a combination of polymer single-crystal templating with SI-ATRP. Reprinted with permission from Zhou et al. [205]

Janus particles have attracted increasing research interest because of the unique properties imparted by their asymmetric structure [39]. One way to synthesize Janus particles is by introducing different polymers onto each side of the particle, thus introducing asymmetric surface properties. Berger et al. used a two-step process involving SI-ATRP followed by a grafting-to approach to immobilize oppositely charged polyelectrolyte brushes on opposite sides of the particles (PAA on one side, poly (2-vinyl pyridine) on the other) [203]. As a result of the pH-responsive nature of the polymer brushes, the resulting Janus particles exhibited pH-responsive aggregation. Liu et al. reported the synthesis of Janus particles via biphasic SI-ATRP at a Pickering emulsion interface [204]. Zhou et al. synthesized Janus particles, with poly(ε-caprolactone) and PNIPAM, through a combination of polymer single-crystal templating and SI-ATRP, as illustrated in Fig. 20 [205].

6 Conclusions

SI-ATRP is a very rapidly developing area of the polymer and materials sciences. The scope of the procedure is constantly evolving, benefiting from new advances in ATRP, such as new catalysts and new initiating techniques, but also from seeking to meet an increasing demand for new advanced nanostructured materials. New ATRP techniques such as eATRP and photoATRP that are mediated by external stimuli have been successfully applied for modification and patterning of surfaces. The modified surfaces can provide extraordinary properties in terms of adhesion, lubrication, antifouling, and antimicrobial behavior. As described in this review, modification of flat, concave, and convex surfaces with polymeric brushes dramatically alters the surface properties of the substrates and provides good dispersibility of

nanoparticles, creates responsiveness in membranes, and provides other properties to composite materials. Although the general polymerization kinetics and mechanisms of homogeneous ATRP and SI-ATRP are similar, there are some peculiarities that can alter the molecular properties of the tethered polymer chains. These differences are based on the specific distribution of active centers anchored to surfaces, diffusion, congestion, and other phenomena. SI-ATRP sometimes resembles other CRP systems but also carries some specific behavior associated with the activator/deactivator nature of ATRP catalysts. Better understanding of such mechanistic features will help in the design and synthesis of new and more efficient hybrid materials.

Acknowledgements Financial supports from NSF (DMR 09 69301), BSF 2012074, DE-EE0006702, and NSERC Discovery Grant (RGPIN/170128-2009) are gratefully acknowledged.

References

1. Braunecker WA, Matyjaszewski K (2007) Controlled/living radical polymerization: features, developments, and perspectives. Prog Polym Sci 32(1):93–146
2. Matyjaszewski K, Davis TP (2002) Handbook of radical polymerization. Wiley-Interscience, Hoboken
3. Matyjaszewski K, Xia JH (2001) Atom transfer radical polymerization. Chem Rev 101(9): 2921–2990
4. Wang JS, Matyjaszewski K (1995) Controlled living radical polymerization – atom-transfer radical polymerization in the presence of transition-metal complexes. J Am Chem Soc 117(20):5614–5615
5. Kamigaito M, Ando T, Sawamoto M (2001) Metal-catalyzed living radical polymerization. Chem Rev 101:3689
6. Matyjaszewski K, Tsarevsky NV (2009) Nanostructured functional materials prepared by atom transfer radical polymerization. Nat Chem 1(4):276–288
7. di Lena F, Matyjaszewski K (2010) Transition metal catalysts for controlled radical polymerization. Prog Polym Sci 35(8):959–1021
8. Shen Y, Tang H, Ding S (2004) Catalyst separation in atom transfer radical polymerization. Prog Polym Sci 29(10):1053–1078
9. Tsarevsky NV, Matyjaszewski K (2007) "Green" atom transfer radical polymerization: from process design to preparation of well-defined environmentally-friendly polymeric materials. Chem Rev 107:2270–2299
10. Jakubowski W, Matyjaszewski K (2006) Activators regenerated by electron transfer for atom-transfer radical polymerization of (meth)acrylates and related block copolymers. Angew Chem Int Ed Engl 45(27):4482–4486
11. Matyjaszewski K, Jakubowski W, Min K, Tang W, Huang JY, Braunecker WA, Tsarevsky NV (2006) Diminishing catalyst concentration in atom transfer radical polymerization with reducing agents. Proc Natl Acad Sci USA 103(42):15309–15314
12. Konkolewicz D, Krys P, Gois JR, Mendonca PV, Zhong M, Wang Y, Gennaro A, Isse AA, Fantin M, Matyjaszewski K (2014) Aqueous RDRP in the presence of Cu0: the exceptional activity of CuI confirms the SARA ATRP mechanism. Macromolecules 47(2):560–570
13. Konkolewicz D, Wang Y, Zhong M, Krys P, Isse AA, Gennaro A, Matyjaszewski K (2013) Reversible-deactivation radical polymerization in the presence of metallic copper.

A critical assessment of the SARA ATRP and SET-LRP mechanisms. Macromolecules 46(22):8749–8772
14. Konkolewicz D, Wang Y, Krys P, Zhong M, Isse AA, Gennaro A, Matyjaszewski K (2014) SARA ATRP or SET-LRP. End of controversy? Polym Chem 5(15):4396–4417
15. Konkolewicz D, Schroder K, Buback J, Bernhard S, Matyjaszewski K (2012) Visible light and sunlight photoinduced ATRP with ppm of Cu catalyst. ACS Macro Lett 1(10):1219–1223
16. Ribelli TG, Konkolewicz D, Bernhard S, Matyjaszewski K (2014) How are radicals (re) generated in photochemical ATRP? J Am Chem Soc 136:13303–13312
17. Fors BP, Hawker CJ (2012) Control of a living radical polymerization of methacrylates by light. Angew Chem Int Ed 51:8850–8853
18. Mosnáček J, Ilčíková M (2012) Photochemically mediated atom transfer radical polymerization of methyl methacrylate using ppm amounts of catalyst. Macromolecules 45(15): 5859–5865
19. Tasdelen MA, Uygun M, Yagci Y (2011) Photoinduced controlled radical polymerization. Macromol Rapid Commun 32(1):58–62
20. Magenau AJD, Strandwitz NC, Gennaro A, Matyjaszewski K (2011) Electrochemically mediated atom transfer radical polymerization. Science 332(6025):81–84
21. Bortolamei N, Isse AA, Magenau AJD, Gennaro A, Matyjaszewski K (2011) Controlled aqueous atom transfer radical polymerization with electrochemical generation of the active catalyst. Angew Chem Int Ed 50(48):11391–11394
22. Magenau AJD, Bortolamei N, Frick E, Park S, Gennaro A, Matyjaszewski K (2013) Investigation of electrochemically mediated atom transfer radical polymerization. Macromolecules 46(11):4346–4353
23. Matyjaszewski K, Tsarevsky NV (2014) Macromolecular engineering by atom transfer radical polymerization. J Am Chem Soc 136:6513–6533
24. Matyjaszewski K (2012) Atom transfer radical polymerization: from mechanisms to applications. Isr J Chem 52(3–4):206–220
25. Matyjaszewski K (2012) Atom transfer radical polymerization (ATRP): current status and future perspectives. Macromolecules 45(10):4015–4039
26. Goto A, Fukuda T (2004) Kinetics of living radical polymerization. Prog Polym Sci 29(4): 329–385
27. Tang W, Matyjaszewski K (2007) Effects of initiator structure on activation rate constants in ATRP. Macromolecules 40(6):1858–1863
28. Tang W, Kwak Y, Braunecker W, Tsarevsky NV, Coote ML, Matyjaszewski K (2008) Understanding atom transfer radical polymerization: effect of ligand and initiator structures on the equilibrium constants. J Am Chem Soc 130(32):10702–10713
29. Tang W, Matyjaszewski K (2006) Effect of ligand structure on activation rate constants in ATRP. Macromolecules 39(15):4953–4959
30. Braunecker WA, Tsarevsky NV, Gennaro A, Matyjaszewski K (2009) Thermodynamic components of the atom transfer radical polymerization equilibrium: quantifying solvent effects. Macromolecules 42(17):6348–6360
31. Seeliger F, Matyjaszewski K (2009) Temperature effect on activation rate constants in ATRP: new mechanistic insights into the activation process. Macromolecules 42(16): 6050–6055
32. Kwiatkowski P, Jurczak J, Pietrasik J, Jakubowski W, Mueller L, Matyjaszewski K (2008) High molecular weight polymethacrylates by AGET ATRP under high pressure. Macromolecules 41(4):1067–1069
33. Pyun J, Matyjaszewski K (2001) Synthesis of nanocomposite organic/inorganic hybrid materials using controlled/"living" radical polymerization. Chem Mater 13(10):3436–3448
34. Hui CM, Pietrasik J, Schmitt M, Mahoney C, Choi J, Bockstaller MR, Matyjaszewski K (2014) Surface-initiated polymerization as an enabling tool for multifunctional (nano-) engineered hybrid materials. Chem Mater 26(1):745–762

35. de Gennes PG (1987) Polymers at an interface: a simplified view. Adv Colloid Interface Sci 27(3–4):189–209
36. Tsujii Y, Ohno K, Yamamoto S, Goto A, Fukuda T (2006) Structure and properties of high-density polymer brushes prepared by surface-initiated living radical polymerization. In: Jordan R (ed) Surface-initiated polymerization I, vol 197. Springer, Berlin/Heidelberg, pp 1–45
37. Kolb HC, Finn MG, Sharpless KB (2001) Click chemistry: diverse chemical function from a few good reactions. Angew Chem Int Ed 40:2004–2021
38. Golas PL, Matyjaszewski K (2010) Marrying click chemistry with polymerization: expanding the scope of polymeric materials. Chem Soc Rev 39(4):1338–1354
39. Walther A, Müller AHE (2013) Janus particles: synthesis, self-assembly, physical properties, and applications. Chem Rev 113(7):5194–5261
40. Yuan J, Xu Y, Walther A, Bolisetty S, Schumacher M, Schmalz H, Ballauff M, Müller AHE (2008) Water-soluble organo-silica hybrid nanowires. Nat Mater 7:718–722
41. Djalali R, Hugenberg N, Fischer K, Schmidt M (1999) Amphipolar core-shell cylindrical brushes. Macromol Rapid Commun 20(8):444–449
42. Djalali R, Li S-Y, Schmidt M (2002) Amphipolar core – shell cylindrical brushes as templates for the formation of gold clusters and nanowires. Macromolecules 35(11):4282–4288
43. Lee H, Jakubowski W, Matyjaszewski K, Yu S, Sheiko SS (2006) Cylindrical core-shell brushes prepared by a combination of ROP and ATRP. Macromolecules 39(15):4983–4989
44. Lee H-I, Pietrasik J, Sheiko SS, Matyjaszewski K (2010) Stimuli-responsive molecular brushes. Prog Polym Sci 35(1–2):24–44
45. Sheiko SS, Sumerlin BS, Matyjaszewski K (2008) Cylindrical molecular brushes: synthesis, characterization, and properties. Prog Polym Sci 33(7):759–785
46. Gao H, Ohno S, Matyjaszewski K (2006) Low polydispersity star polymers via cross-linking macromonomers by ATRP. J Am Chem Soc 128(47):15111–15113
47. Gao H, Matyjaszewski K (2009) Synthesis of functional polymers with controlled architecture by CRP of monomers in the presence of cross-linkers: from stars to gels. Prog Polym Sci 34(4):317–350
48. Müllner M, Lunkenbein T, Schieder M, Gröschel AH, Miyajima N, Förtsch M, Breu J, Caruso F, Müller AHE (2012) Template-directed mild synthesis of anatase hybrid nanotubes within cylindrical core–shell–corona polymer brushes. Macromolecules 45(17):6981–6988
49. Müllner M, Lunkenbein T, Miyajima N, Breu J, Müller AHE (2012) A facile polymer templating route toward high-aspect-ratio crystalline titania nanostructures. Small 8(17): 2636–2640
50. Connal LA, Franks GV, Qiao GG (2010) Photochromic, metal-absorbing honeycomb structures. Langmuir 26(13):10397–10400
51. Pang X, Zhao L, Han W, Xin X, Lin Z (2013) A general and robust strategy for the synthesis of nearly monodisperse colloidal nanocrystals. Nat Nano 8(6):426–431
52. Kruk M, Dufour B, Celer EB, Kowalewski T, Jaroniec M, Matyjaszewski K (2008) Grafting monodisperse polymer chains from concave surfaces of ordered mesoporous silicas. Macromolecules 41(22):8584–8591
53. Mori H, Seng DC, Zhang M, Mueller AHE (2002) Hybrid nanoparticles with hyperbranched polymer shells via self-condensing atom transfer radical polymerization from silica surfaces. Langmuir 18(9):3682–3693
54. Dong H, Zhu M, Yoon JA, Gao H, Jin R, Matyjaszewski K (2008) One-pot synthesis of robust core/shell gold nanoparticles. J Am Chem Soc 130(39):12852–12853
55. Ye P, Dong H, Zhong M, Matyjaszewski K (2011) Synthesis of binary polymer brushes via two-step reverse atom transfer radical polymerization. Macromolecules 44(7):2253–2260
56. Luzinov I, Minko S, Tsukruk VV (2004) Adaptive and responsive surfaces through controlled reorganization of interfacial polymer layers. Prog Polym Sci 29(7):635–698
57. Julthongpiput D, Lin Y-H, Teng J, Zubarev ER, Tsukruk VV (2003) Y-shaped polymer brushes: nanoscale switchable surfaces. Langmuir 19(19):7832–7836

58. Zhao B, He T (2003) Synthesis of well-defined mixed poly(methyl methacrylate)/polystyrene brushes from an asymmetric difunctional initiator-terminated self-assembled monolayer. Macromolecules 36(23):8599–8602
59. Li Y, Tao P, Viswanath A, Benicewicz BC, Schadler LS (2012) Bimodal surface ligand engineering: the key to tunable nanocomposites. Langmuir 29(4):1211–1220
60. Chen R, Feng W, Zhu S, Botton G, Ong B, Wu Y (2006) Surface-initiated atom transfer radical polymerization grafting of poly(2,2,2-trifluoroethyl methacrylate) from flat silicon wafer surfaces. J Polym Sci A Polym Chem 44(3):1252–1262
61. Feng W, Chen R, Brash JL, Zhu S (2005) Surface-initiated atom transfer radical polymerization of oligo(ethylene glycol) methacrylate: effect of solvent on graft density. Macromol Rapid Commun 26(17):1383–1388
62. Ell JR, Mulder DE, Faller R, Patten TE, Kuhl TL (2009) Structural determination of high density, ATRP grown polystyrene brushes by neutron reflectivity. Macromolecules 42(24):9523–9527
63. Tomlinson MR, Efimenko K, Genzer J (2006) Study of kinetics and macroinitiator efficiency in surface-initiated atom-transfer radical polymerization. Macromolecules 39(26):9049–9056
64. Wang S, Zhu Y (2009) Facile method to prepare smooth and homogeneous polymer brush surfaces of varied brush thickness and grafting density. Langmuir 25(23):13448–13455
65. Jones DM, Brown AA, Huck WTS (2002) Surface-initiated polymerizations in aqueous media: effect of initiator density. Langmuir 18(4):1265–1269
66. Bao Z, Bruening ML, Baker GL (2006) Control of the density of polymer brushes prepared by surface-initiated atom transfer radical polymerization. Macromolecules 39(16):5251–5258
67. Jia H, Wildes A, Titmuss S (2012) Structure of pH-responsive polymer brushes grown at the gold–water interface: dependence on grafting density and temperature. Macromolecules 45(1):305–312
68. Behling RE, Williams BA, Staade BL, Wolf LM, Cochran EW (2009) Influence of graft density on kinetics of surface-initiated ATRP of polystyrene from montmorillonite. Macromolecules 42(6):1867–1872
69. Lego B, François M, Skene WG, Giasson S (2009) Polymer brush covalently attached to OH-functionalized mica surface via surface-initiated ATRP: control of grafting density and polymer chain length. Langmuir 25(9):5313–5321
70. Wu T, Efimenko K, Vlček P, Šubr V, Genzer J (2003) Formation and properties of anchored polymers with a gradual variation of grafting densities on flat substrates. Macromolecules 36(7):2448–2453
71. Lilge I, Steuber M, Tranchida D, Sperotto E, Schönherr H (2013) Tailored (Bio)interfaces via surface initiated polymerization: control of grafting density and new responsive diblock copolymer brushes. Macromol Symp 328(1):64–72
72. Coad BR, Styan KE, Meagher L (2014) One step ATRP initiator immobilization on surfaces leading to gradient-grafted polymer brushes. ACS Appl Mater Interfaces 6(10):7782–7789
73. Ohno K, Morinaga T, Koh K, Tsujii Y, Fukuda T (2005) Synthesis of monodisperse silica particles coated with well-defined, high-density polymer brushes by surface-initiated atom transfer radical polymerization. Macromolecules 38(6):2137–2142
74. Huang C, Tassone T, Woodberry K, Sunday D, Green DL (2009) Impact of ATRP initiator spacer length on grafting poly(methyl methacrylate) from silica nanoparticles. Langmuir 25(23):13351–13360
75. Sunday D, Curras-Medina S, Green DL (2010) Impact of initiator spacer length on grafting polystyrene from silica nanoparticles. Macromolecules 43(11):4871–4878
76. Pietrasik J, Hui CM, Chaladaj W, Dong H, Choi J, Jurczak J, Bockstaller MR, Matyjaszewski K (2011) Silica-polymethacrylate hybrid particles synthesized using high-pressure atom transfer radical polymerization. Macromol Rapid Commun 32(3):295–301
77. Pyun J, Jia S, Kowalewski T, Patterson GD, Matyjaszewski K (2003) Synthesis and characterization of organic/inorganic hybrid nanoparticles: kinetics of surface-initiated

atom transfer radical polymerization and morphology of hybrid nanoparticle ultrathin films. Macromolecules 36(14):5094–5104
78. El Harrak A, Carrot G, Oberdisse J, Eychenne-Baron C, Boué F (2004) Surface−atom transfer radical polymerization from silica nanoparticles with controlled colloidal stability. Macromolecules 37(17):6376–6384
79. Tchoul MN, Dalton M, Tan L-S, Dong H, Hui CM, Matyjaszewski K, Vaia RA (2012) Enhancing the fraction of grafted polystyrene on silica hybrid nanoparticles. Polymer 53(1): 79–86
80. Averick SE, Bazewicz CG, Woodman BF, Simakova A, Mehl RA, Matyjaszewski K (2013) Protein–polymer hybrids: conducting ARGET ATRP from a genetically encoded cleavable ATRP initiator. Eur Polym J 49(10):2919–2924
81. Sugnaux C, Lavanant L, Klok H-A (2013) Aqueous fabrication of pH-gated, polymer-brush-modified alumina hybrid membranes. Langmuir 29(24):7325–7333
82. Cheng N, Azzaroni O, Moya S, Huck WTS (2006) The effect of [CuI]/[CuII] ratio on the kinetics and conformation of polyelectrolyte brushes by atom transfer radical polymerization. Macromol Rapid Commun 27(19):1632–1636
83. Kim J-B, Bruening ML, Baker GL (2000) Surface-initiated atom transfer radical polymerization on gold at ambient temperature. J Am Chem Soc 122(31):7616–7617
84. Shah RR, Merreceyes D, Husemann M, Rees I, Abbott NL, Hawker CJ, Hedrick JL (2000) Using atom transfer radical polymerization to amplify monolayers of initiators patterned by microcontact printing into polymer brushes for pattern transfer. Macromolecules 33(2): 597–605
85. Hou J, Shi Q, Stagnaro P, Ye W, Jin J, Conzatti L, Yin J (2013) Aqueous-based immobilization of initiator and surface-initiated ATRP to construct hemocompatible surface of poly (styrene-b-(ethylene-co-butylene)-b-styrene) elastomer. Colloids Surf B Biointerfaces 111:333–341
86. Chakkalakal GL, Alexandre M, Abetz C, Boschetti-de-Fierro A, Abetz V (2012) Surface-initiated controlled radical polymerization from silica nanoparticles with high initiator density. Macromol Chem Phys 213(5):513–528
87. Bombalski L, Min K, Dong H, Tang C, Matyjaszewski K (2007) Preparation of well-defined hybrid materials by ATRP in miniemulsion. Macromolecules 40(21):7429–7432
88. Audouin F, Blas H, Pasetto P, Beaunier P, Boissière C, Sanchez C, Save M, Charleux B (2008) Structured hybrid nanoparticles via surface-initiated ATRP of methyl methacrylate from ordered mesoporous silica. Macromol Rapid Commun 29(11):914–921
89. Pasetto P, Blas H, Audouin F, Boissière C, Sanchez C, Save M, Charleux B (2009) Mechanistic insight into surface-initiated polymerization of methyl methacrylate and styrene via ATRP from ordered mesoporous silica particles. Macromolecules 42(16):5983–5995
90. Liu H, Zhu Y-L, Zhang J, Lu Z-Y, Sun Z-Y (2012) Influence of grafting surface curvature on chain polydispersity and molecular weight in concave surface-initiated polymerization. ACS Macro Lett 1(11):1249–1253
91. Gao X, Feng W, Zhu S, Sheardown H, Brash JL (2010) Kinetic modeling of surface-initiated atom transfer radical polymerization. Macromol React Eng 4(3–4):235–250
92. Turgman-Cohen S, Genzer J (2011) Simultaneous bulk- and surface-initiated controlled radical polymerization from planar substrates. J Am Chem Soc 133(44):17567–17569
93. Turgman-Cohen S, Genzer J (2012) Computer simulation of concurrent bulk- and surface-initiated living polymerization. Macromolecules 45(4):2128–2137
94. Schneider D, Schmitt M, Hui CM, Sainidou R, Rembert P, Matyjaszewski K, Bockstaller MR, Fytas G (2014) Role of polymer graft architecture on the acoustic eigenmode formation in densely polymer-tethered colloidal particles. ACS Macro Lett 3(10):1059–1063
95. Mastan E, Xi L, Zhu S (2015) What limits the chain growth from flat surfaces in surface-initiated ATRP: propagation, termination or both? Macromol Theor Simulat 24(2):89–99. doi:10.1002/mats.201400085

96. Huang W, Kim J-B, Bruening ML, Baker GL (2002) Functionalization of surfaces by water-accelerated atom-transfer radical polymerization of hydroxyethyl methacrylate and subsequent derivatization. Macromolecules 35(4):1175–1179
97. Dunderdale GJ, Urata C, Miranda DF, Hozumi A (2014) Large-scale and environmentally friendly synthesis of pH-responsive oil-repellent polymer brush surfaces under ambient conditions. ACS Appl Mater Interfaces 6(15):11864–11868
98. Jain P, Dai J, Baker GL, Bruening ML (2008) Rapid synthesis of functional polymer brushes by surface-initiated atom transfer radical polymerization of an acidic monomer. Macromolecules 41(22):8413–8417
99. Matyjaszewski K, Miller PJ, Shukla N, Immaraporn B, Gelman A, Luokala BB, Siclovan TM, Kickelbick G, Vallant T, Hoffmann H, Pakula T (1999) Polymers at interfaces: using atom transfer radical polymerization in the controlled growth of homopolymers and block copolymers from silicon surfaces in the absence of untethered sacrificial initiator. Macromolecules 32(26):8716–8724
100. Feng W, Brash J, Zhu S (2004) Atom-transfer radical grafting polymerization of 2-methacryloyloxyethyl phosphorylcholine from silicon wafer surfaces. J Polym Sci A Polym Chem 42(12):2931–2942
101. Xiao D, Wirth MJ (2002) Kinetics of surface-initiated atom transfer radical polymerization of acrylamide on silica. Macromolecules 35(8):2919–2925
102. Zhou D, Gao X, Wang W-J, Zhu S (2012) Termination of surface radicals and kinetic modeling of ATRP grafting from flat surfaces by addition of deactivator. Macromolecules 45(3):1198–1207
103. Kim J-B, Huang W, Miller MD, Baker GL, Bruening ML (2003) Kinetics of surface-initiated atom transfer radical polymerization. J Polym Sci A Polym Chem 41(3):386–394
104. Wang Y, Soerensen N, Zhong M, Schroeder H, Buback M, Matyjaszewski K (2013) Improving the "livingness" of ATRP by reducing Cu catalyst concentration. Macromolecules 46(3):683–691
105. Koylu D, Carter KR (2009) Stimuli-responsive surfaces utilizing cleavable polymer brush layers. Macromolecules 42(22):8655–8660
106. Yamamoto K, Miwa Y, Tanaka H, Sakaguchi M, Shimada S (2002) Living radical graft polymerization of methyl methacrylate to polyethylene film with typical and reverse atom transfer radical polymerization. J Polym Sci A Polym Chem 40(20):3350–3359
107. Kang C, Crockett RM, Spencer ND (2014) Molecular-weight determination of polymer brushes generated by SI-ATRP on flat surfaces. Macromolecules 47(1):269–275
108. Devaux C, Chapel JP, Beyou E, Chaumont P (2002) Controlled structure and density of "living" polystyrene brushes on flat silica surfaces. Eur Phys J E 7:345–352
109. Miwa Y, Yamamoto K, Sakaguchi M, Shimada S (2001) Well-defined polystyrene grafted to polypropylene backbone by "living" radical polymerization with TEMPO. Macromolecules 34(7):2089–2094
110. Yamago S, Yahata Y, Nakanishi K, Konishi S, Kayahara E, Nomura A, Goto A, Tsujii Y (2013) Synthesis of concentrated polymer brushes via surface-initiated organotellurium-mediated living radical polymerization. Macromolecules 46(17):6777–6785
111. Ohno K, Akashi T, Huang Y, Tsujii Y (2010) Surface-initiated living radical polymerization from narrowly size-distributed silica nanoparticles of diameters less than 100 nm. Macromolecules 43(21):8805–8812
112. Ohno K, Tabata H, Tsujii Y (2013) Surface-initiated living radical polymerization from silica particles functionalized with poly(ethylene glycol)-carrying initiator. Colloid Polym Sci 291(1):127–135
113. Gorman CB, Petrie RJ, Genzer J (2008) Effect of substrate geometry on polymer molecular weight and polydispersity during surface-initiated polymerization. Macromolecules 41(13): 4856–4865
114. Fischer H (1997) The persistent radical effect in "living" radical polymerization. Macromolecules 30(19):5666–5672

115. Matyjaszewski K (1997) Mechanistic and synthetic aspects of atom transfer radical polymerization. J Macromol Sci A Pure Appl Chem 34(10):1785–1801
116. Fukuda T, Goto A (1997) Gel permeation chromatographic determination of activation rate constants in nitroxide-controlled free radical polymerization, 2. Analysis of evolution of polydispersities. Macromol Rapid Commun 18(8):683–688
117. Ejaz M, Yamamoto S, Ohno K, Tsujii Y, Fukuda T (1998) Controlled graft polymerization of methyl methacrylate on silicon substrate by the combined use of the langmuir−blodgett and atom transfer radical polymerization techniques. Macromolecules 31(17):5934–5936
118. Jeyaprakash JD, Samuel S, Dhamodharan R, Rühe J (2002) Polymer brushes via ATRP: role of activator and deactivator in the surface-initiated ATRP of styrene on planar substrates. Macromol Rapid Commun 23(4):277–281
119. Chen R, Feng W, Zhu S, Botton G, Ong B, Wu Y (2006) Surface-initiated atom transfer radical polymerization of polyhedral oligomeric silsesquioxane (POSS) methacrylate from flat silicon wafer. Polymer 47(4):1119–1123
120. Li B, Yu B, Huck WTS, Liu W, Zhou F (2013) Electrochemically mediated atom transfer radical polymerization on nonconducting substrates: controlled brush growth through catalyst diffusion. J Am Chem Soc 135(5):1708–1710
121. Huang J, Pintauer T, Matyjaszewski K (2004) Effect of variation of [PMDETA]0/[Cu(I)Br] 0 ratio on atom transfer radical polymerization ofn-butyl acrylate. J Polym Sci A Polym Chem 42(13):3285–3292
122. Sharma R, Goyal A, Caruthers JM, Won Y-Y (2006) Inhibitive chain transfer to ligand in the ATRP of *n*-butyl acrylate. Macromolecules 39(14):4680–4689
123. Yu Q, Zhang Y, Chen H, Wu Z, Huang H, Cheng C (2010) Protein adsorption on poly (N-isopropylacrylamide)-modified silicon surfaces: effects of grafted layer thickness and protein size. Colloids Surf B Biointerfaces 76(2):468–474
124. Wang XJ, Bohn PW (2007) Spatiotemporally controlled formation of two-component counter-propagating lateral graft density gradients of mixed polymer brushes on planar Au surfaces. Adv Mater 19(4):515–520
125. Xue C, Yonet-Tanyeri N, Brouette N, Sferrazza M, Braun PV, Leckband DE (2011) Protein adsorption on poly(N-isopropylacrylamide) brushes: dependence on grafting density and chain collapse. Langmuir 27(14):8810–8818
126. Liu X, Ye Q, Yu B, Liang Y, Liu W, Zhou F (2010) Switching water droplet adhesion using responsive polymer brushes. Langmuir 26(14):12377–12382
127. Hui CM, Dang A, Chen B, Yan J, Konkolewicz D, He H, Ferebee R, Bockstaller MR, Matyjaszewski K (2014) Effect of thermal self-initiation on the synthesis, composition, and properties of particle brush materials. Macromolecules 47(16):5501–5508
128. Mu B, Shen R, Liu P (2009) Crosslinked polymeric nanocapsules from polymer brushes grafted silica nanoparticles via surface-initiated atom transfer radical polymerization. Colloids Surf B Biointerfaces 74(2):511–515
129. Wu D, Hui CM, Dong H, Pietrasik J, He H, Ryu HJ, Li Z, Zhong M, Jaroniec M, Kowalewski T, Matyjaszewski K (2011) Nanonetwork-structured polystyrene and carbon materials with core-shell nanosphere network unit. Polym Preprints 52(2):693–694
130. Yamamoto S, Ejaz M, Tsujii Y, Fukuda T (2000) Surface interaction forces of well-defined, high-density polymer brushes studied by atomic force microscopy. 2. Effect of graft density. Macromolecules 33(15):5608–5612
131. Liao W-P, Elliott IG, Faller R, Kuhl TL (2013) Normal and shear interactions between high grafting density polymer brushes grown by atom transfer radical polymerization. Soft Matter 9(24):5753–5761
132. Xu FJ, Neoh KG, Kang ET (2009) Bioactive surfaces and biomaterials via atom transfer radical polymerization. Prog Polym Sci 34(8):719–761
133. Krishnamoorthy M, Hakobyan S, Ramstedt M, Gautrot JE (2014) Surface-initiated polymer brushes in the biomedical field: applications in membrane science, biosensing, cell culture, regenerative medicine and antibacterial coatings. Chem Rev 114(21):10976–11026

134. Jiang H, Xu F-J (2013) Biomolecule-functionalized polymer brushes. Chem Soc Rev 42(8): 3394
135. Barbey R, Lavanant L, Paripovic D, Schüwer N, Sugnaux C, Tugulu S, Klok H-A (2009) Polymer brushes via surface-initiated controlled radical polymerization: synthesis, characterization, properties, and applications. Chem Rev 109(11):5437–5527
136. Siegwart DJ, Oh JK, Matyjaszewski K (2012) ATRP in the design of functional materials for biomedical applications. Prog Polym Sci 37(1):18–37
137. Yu K, Mei Y, Hadjesfandiari N, Kizhakkedathu JN (2014) Engineering biomaterials surfaces to modulate the host response. Colloids Surf B Biointerfaces 124:69–79
138. Zhang L, Ning C, Zhou T, Liu X, Yeung KWK, Zhang T, Xu Z, Wang X, Wu S, Chu PK (2014) Polymeric nanoarchitectures on Ti-based implants for antibacterial applications. ACS Appl Mater Interfaces 6(20):17323–17345
139. Feng W, Brash JL, Zhu S (2006) Non-biofouling materials prepared by atom transfer radical polymerization grafting of 2-methacryloloxyethyl phosphorylcholine: separate effects of graft density and chain length on protein repulsion. Biomaterials 27(6):847–855
140. Feng W, Zhu S, Ishihara K, Brash JL (2005) Adsorption of fibrinogen and lysozyme on silicon grafted with poly(2-methacryloyloxyethyl phosphorylcholine) via surface-initiated atom transfer radical polymerization. Langmuir 21(13):5980–5987
141. Gao X, Feng W, Zhu S, Sheardown H, Brash JL (2008) A facile method of forming nanoscale patterns on poly(ethylene glycol)-based surfaces by self-assembly of randomly grafted block copolymer brushes. Langmuir 24(15):8303–8308
142. Gao X, Kučerka N, Nieh M-P, Katsaras J, Zhu S, Brash JL, Sheardown H (2009) Chain conformation of a new class of PEG-based thermoresponsive polymer brushes grafted on silicon as determined by neutron reflectometry. Langmuir 25(17):10271–10278
143. Feng W, Zhu S, Brash JL (2005) Preparation of biocompatible surfaces by atom transfer radical polymerization grafting and evaluation of protein adsorption. Polym Preprints 46(2): 1278
144. Gao X, Zhu S, Sheardown H, Brash JL (2010) Nanoscale patterning through self-assembly of hydrophilic block copolymers with one chain end constrained to surface. Polymer 51(8): 1771–1778
145. Feng W, Brash JL, Zhu S (2005) Atom transfer radical polymerization grafting of 2-methacryloyloxyethyl phosphorylcholine for non-biofouling surfaces. Polym Preprints 46(2):154
146. Feng W, Gao X, McClung G, Zhu S, Ishihara K, Brash JL (2011) Methacrylate polymer layers bearing poly(ethylene oxide) and phosphorylcholine side chains as non-fouling surfaces: in vitro interactions with plasma proteins and platelets. Acta Biomater 7(10): 3692–3699
147. Feng W, Zhu S, Ishihara K, Brash JL (2006) Protein resistant surfaces: comparison of acrylate graft polymers bearing oligo-ethylene oxide and phosphorylcholine side chains. Biointerphases 1(1):50
148. Zhu S, Brash JL, Feng W (2007) Atom transfer radical polymerization grafting for surface modification-high grafting density and controlled molecular weight. In: Proceedings 2007 annual meeting of the American Institute of Chemical Engineers (07AIChE). AIChE, Salt Lake City. Paper ID 101135
149. Feng W, Nieh M-P, Zhu S, Harroun TA, Katsaras J, Brash JL (2007) Characterization of protein resistant, grafted methacrylate polymer layers bearing oligo(ethylene glycol) and phosphorylcholine side chains by neutron reflectometry. Biointerphases 2(1):34
150. Jin Z, Brash JL, Zhu S (2010) ATRP grafting of oligo(ethylene glycol) methacrylates from gold surface — effect of monomer size on grafted chain and EO unit densities. Can J Chem 88(5):411–417
151. Jin Z, Feng W, Beisser K, Zhu S, Sheardown H, Brash JL (2009) Protein-resistant polyurethane prepared by surface-initiated atom transfer radical graft polymerization (ATRgP) of

water-soluble polymers: effects of main chain and side chain lengths of grafts. Colloids Surf B Biointerfaces 70(1):53–59
152. Jin Z, Feng W, Zhu S, Sheardown H, Brash JL (2009) Protein-resistant polyurethane via surface-initiated atom transfer radical polymerization of oligo(ethylene glycol) methacrylate. J Biomed Mater Res A 91A(4):1189–1201
153. Jin Z, Feng W, Zhu S, Sheardown H, Brash JL (2010) Protein-resistant polyurethane by sequential grafting of poly(2-hydroxyethyl methacrylate) and poly(oligo(ethylene glycol) methacrylate) via surface-initiated ATRP. J Biomed Mater Res A 95(4):1223–1232
154. Jin Z, Feng W, Zhu S, Sheardown H, Brash JL (2010) Protein-resistant materials via surface-initiated atom transfer radical polymerization of 2-methacryloyloxyethyl phosphorylcholine. J Biomater Sci Polym Ed 21(10):1331–1344
155. Yu B-Y, Zheng J, Chang Y, Sin M-C, Chang C-H, Higuchi A, Sun Y-M (2014) Surface zwitterionization of titanium for a general Bio-inert control of plasma proteins, blood cells, tissue cells, and bacteria. Langmuir 30(25):7502–7512
156. Sin M-C, Sun Y-M, Chang Y (2014) Zwitterionic-based stainless steel with well-defined polysulfobetaine brushes for general bioadhesive control. ACS Appl Mater Interfaces 6(2): 861–873
157. Lee SB, Koepsel RR, Morley SW, Matyjaszewski K, Sun Y, Russell AJ (2004) Permanent, nonleaching antibacterial surfaces. 1. Synthesis by atom transfer radical polymerization. Biomacromolecules 5(3):877–882
158. Huang J, Murata H, Koepsel RR, Russell AJ, Matyjaszewski K (2007) Antibacterial polypropylene via surface-initiated atom transfer radical polymerization. Biomacromolecules 8(5):1396–1399
159. Yu Q, Cho J, Shivapooja P, Ista LK, López GP (2013) Nanopatterned smart polymer surfaces for controlled attachment, killing, and release of bacteria. ACS Appl Mater Interfaces 5(19): 9295–9304
160. Kobayashi M, Terada M, Takahara A (2012) Polyelectrolyte brushes: a novel stable lubrication system in aqueous conditions. Faraday Discuss 156:403
161. Kobayashi M, Terayama Y, Hosaka N, Kaido M, Suzuki A, Yamada N, Torikai N, Ishihara K, Takahara A (2007) Friction behavior of high-density poly(2-methacryloyloxyethyl phosphorylcholine) brush in aqueous media. Soft Matter 3(6):740
162. Chen M, Briscoe WH, Armes SP, Klein J (2009) Lubrication at physiological pressures by polyzwitterionic brushes. Science 323(5922):1698–1701
163. Nomura A, Okayasu K, Ohno K, Fukuda T, Tsujii Y (2011) Lubrication mechanism of concentrated polymer brushes in solvents: effect of solvent quality and thereby swelling state. Macromolecules 44(12):5013–5019
164. Bielecki RM, Benetti EM, Kumar D, Spencer ND (2012) Lubrication with oil-compatible polymer brushes. Tribol Lett 45(3):477–487
165. Kumar S, Dory YL, Lepage M, Zhao Y (2011) Surface-grafted stimuli-responsive block copolymer brushes for the thermo-, photo- and pH-sensitive release of dye molecules. Macromolecules 44(18):7385–7393
166. Kumar S, Tong X, Dory YL, Lepage M, Zhao Y (2013) A CO2-switchable polymer brush for reversible capture and release of proteins. Chem Commun 49(1):90–92
167. Wischerhoff E, Uhlig K, Lankenau A, Börner HG, Laschewsky A, Duschl C, Lutz JF (2008) Controlled cell adhesion on PEG-based switchable surfaces. Angew Chem Int Ed 47(30): 5666–5668
168. Kobayashi M, Terada M, Takahara A (2011) Reversible adhesive-free nanoscale adhesion utilizing oppositely charged polyelectrolyte brushes. Soft Matter 7(12):5717
169. Kobayashi M, Takahara A (2013) Environmentally friendly repeatable adhesion using a sulfobetaine-type polyzwitterion brush. Polym Chem 4(18):4987
170. Matrab T, Save M, Charleux B, Pinson J, Cabet-deliry E, Adenier A, Chehimi MM, Delamar M (2007) Grafting densely-packed poly(n-butyl methacrylate) chains from an iron substrate by aryl diazonium surface-initiated ATRP: XPS monitoring. Surf Sci 601(11):2357–2366

171. Gong R, Maclaughlin S, Zhu S (2008) Surface modification of active metals through atom transfer radical polymerization grafting of acrylics. Appl Surf Sci 254(21):6802–6809
172. Chen R, Zhu S, Maclaughlin S (2008) Grafting acrylic polymers from flat nickel and copper surfaces by surface-initiated atom transfer radical polymerization. Langmuir 24(13): 6889–6896
173. Lu G, Li Y-M, Lu C-H, Xu Z-Z (2010) Corrosion protection of iron surface modified by poly(methyl methacrylate) using surface-initiated atom transfer radical polymerization (SI-ATRP). Colloid Polym Sci 288(14–15):1445–1455
174. Xie Z, Chen C, Zhou X, Gao T, Liu D, Miao Q, Zheng Z (2014) Massively parallel patterning of complex 2D and 3D functional polymer brushes by polymer pen lithography. ACS Appl Mater Interfaces 6(15):11955–11964
175. Ohno K, Kayama Y, Ladmiral V, Fukuda T, Tsujii Y (2010) A versatile method of initiator fixation for surface-initiated living radical polymerization on polymeric substrates. Macromolecules 43(13):5569–5574
176. Sweat DP, Kim M, Yu X, Schmitt SK, Han E, Choi JW, Gopalan P (2013) A dual functional layer for block copolymer self-assembly and the growth of nanopatterned polymer brushes. Langmuir 29(41):12858–12865
177. Chen T, Amin I, Jordan R (2012) Patterned polymer brushes. Chem Soc Rev 41(8):3280
178. Yue W-W, Li H-J, Xiang T, Qin H, Sun S-D, Zhao C-S (2013) Grafting of zwitterion from polysulfone membrane via surface-initiated ATRP with enhanced antifouling property and biocompatibility. J Membr Sci 446:79–91
179. Frost S, Ulbricht M (2013) Thermoresponsive ultrafiltration membranes for the switchable permeation and fractionation of nanoparticles. J Membr Sci 448:1–11
180. Chen Y-C, Xie R, Chu L-Y (2013) Stimuli-responsive gating membranes responding to temperature, pH, salt concentration and anion species. J Membr Sci 442:206–215
181. Ran J, Wu L, Zhang Z, Xu T (2014) Atom transfer radical polymerization (ATRP): a versatile and forceful tool for functional membranes. Prog Polym Sci 39(1):124–144
182. Slowing II, Trewyn BG, Giri S, Lin VSY (2007) Mesoporous silica nanoparticles for drug delivery and biosensing applications. Adv Funct Mater 17(8):1225–1236
183. Zhou Z, Zhu S, Zhang D (2007) Grafting of thermo-responsive polymer inside mesoporous silica with large pore size using ATRP and investigation of its use in drug release. J Mater Chem 17(23):2428–2433
184. Shen Y, Qi L, Wei X, Zhang R, Mao L (2011) Preparation of well-defined environmentally responsive polymer brushes on monolithic surface by two-step atom transfer radical polymerization method for HPLC. Polymer 52(17):3725–3731
185. Zhu Y, Xu X, Brault ND, Keefe AJ, Han X, Deng Y, Xu J, Yu Q, Jiang S (2014) Cellulose paper sensors modified with zwitterionic poly(carboxybetaine) for sensing and detection in complex media. Anal Chem 86(6):2871–2875
186. He H, Zhong M, Konkolewicz D, Yacatto K, Rappold T, Sugar G, David NE, Matyjaszewski K (2013) Carbon black functionalized with hyperbranched polymers: synthesis, characterization, and application in reversible CO_2 capture. J Mater Chem A 1(23):6810
187. Choi J, Hui CM, Schmitt M, Pietrasik J, Margel S, Matyjazsewski K, Bockstaller MR (2013) Effect of polymer-graft modification on the order formation in particle assembly structures. Langmuir 29(21):6452–6459
188. Choi J, Hui CM, Pietrasik J, Dong H, Matyjaszewski K, Bockstaller MR (2012) Toughening fragile matter: mechanical properties of particle solids assembled from polymer-grafted hybrid particles synthesized by ATRP. Soft Matter 8(15):4072–4082
189. Dang A, Hui CM, Ferebee R, Kubiak J, Li T, Matyjaszewski K, Bockstaller MR (2013) Thermal properties of particle brush materials: effect of polymer graft architecture on the glass transition temperature in polymer-grafted colloidal systems. Macromol Symp 331–332 (1):9–16

190. Dang A, Ojha SS, Hui CM, Mahoney C, Matyjaszewski K, Bockstaller MR (2014) High transparency polymer nanocomposites enabled by polymer graft modification of particle fillers. Langmuir 30(48):14434–14442
191. Pyun J (2007) Nanocomposite materials from functional polymers and magnetic colloids. Polym Rev 47(2):231–263
192. Bull MM, Chung WJ, Anderson SR, Kim S-J, Shim I-B, Paik H-J, Pyun J (2010) Synthesis of ferromagnetic polymer coated nanoparticles on multi-gram scale with tunable particle size. J Mater Chem 20(29):6023
193. Marutani E, Yamamoto S, Ninjbadgar T, Tsujii Y, Fukuda T, Takano M (2004) Surface-initiated atom transfer radical polymerization of methyl methacrylate on magnetite nanoparticles. Polymer 45(7):2231–2235
194. Zeltner M, Grass RN, Schaetz A, Bubenhofer SB, Luechinger NA, Stark WJ (2012) Stable dispersions of ferromagnetic carbon-coated metal nanoparticles: preparation via surface initiated atom transfer radical polymerization. J Mater Chem 22(24):12064
195. Chen R, Maclaughlin S, Botton G, Zhu S (2009) Preparation of Ni-g-polymer core–shell nanoparticles by surface-initiated atom transfer radical polymerization. Polymer 50(18): 4293–4298
196. Gu H, Faucher S, Zhu S (2012) Magnetic organosilica nanoparticles for localized polymer surface modification. Macromol Mater Eng 297(3):263–271
197. Liu G, Cai M, Wang X, Zhou F, Liu W (2014) Core–shell–corona-structured polyelectrolyte brushes-grafting magnetic nanoparticles for water harvesting. ACS Appl Mater Interfaces 6(14):11625–11632
198. Dong H, Huang J, Koepsel RR, Ye P, Russell AJ, Matyjaszewski K (2011) Recyclable antibacterial magnetic nanoparticles grafted with quaternized poly(2-(dimethylamino)ethyl methacrylate) brushes. Biomacromolecules 12(4):1305–1311
199. Zeltner M, Toedtli LM, Hild N, Fuhrer R, Rossier M, Gerber LC, Raso RA, Grass RN, Stark WJ (2013) Ferromagnetic inks facilitate large scale paper recycling and reduce bleach chemical consumption. Langmuir 29(16):5093–5098
200. Tian C, Bao C, Binder A, Zhu Z, Hu B, Guo Y, Zhao B, Dai S (2013) An efficient and reusable "hairy" particle acid catalyst for the synthesis of 5-hydroxymethylfurfural from dehydration of fructose in water. Chem Commun 49(77):8668–8670
201. Farmer SC, Patten TE (2001) Photoluminescent polymer/quantum dot composite nanoparticles. Chem Mater 13(11):3920–3926
202. Esteves ACC, Bombalski L, Trindade T, Matyjaszewski K, Barros-Timmons A (2007) Polymer grafting from CdS quantum dots via AGET ATRP in miniemulsion. Small 3(7): 1230–1236
203. Berger S, Synytska A, Ionov L, Eichhorn K-J, Stamm M (2008) Stimuli-responsive bi-component polymer janus particles by "grafting from"/"grafting to" approaches. Macromolecules 41(24):9669–9676
204. Liu B, Wei W, Qu X, Yang Z (2008) Janus colloids formed by biphasic grafting at a pickering emulsion interface. Angew Chem Int Ed 47(21):3973–3975
205. Zhou T, Wang B, Dong B, Li CY (2012) Thermoresponsive amphiphilic janus silica nanoparticles via combining "polymer single-crystal templating" and "grafting-from" methods. Macromolecules 45(21):8780–8789